Provided for non-commercial research and education use.
Not for reproduction, distribution or commercial use.

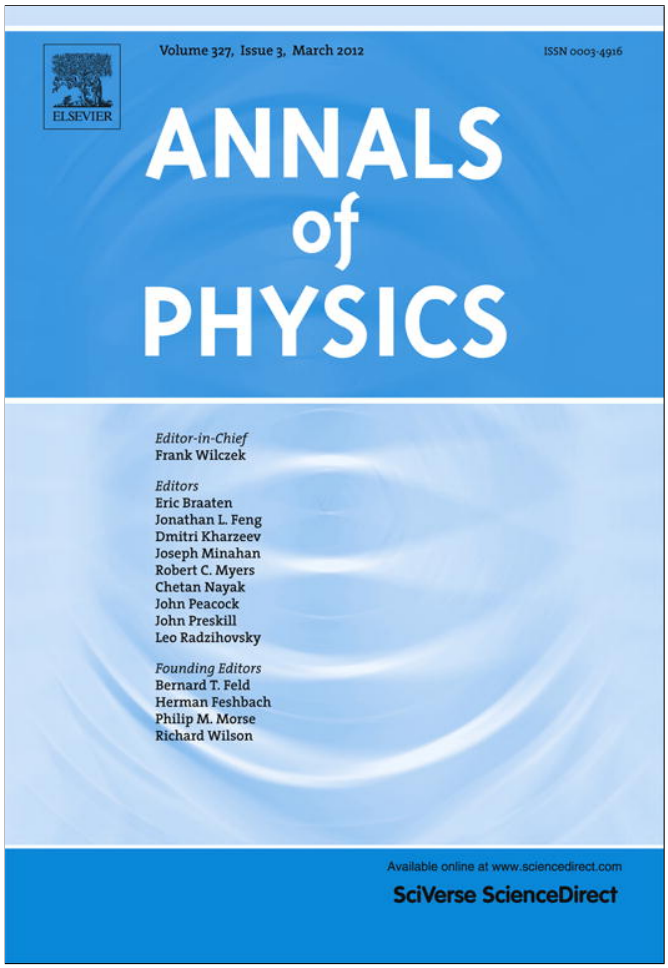

This article appeared in a journal published by Elsevier. The attached copy is furnished to the author for internal non-commercial research and education use, including for instruction at the authors institution and sharing with colleagues.

Other uses, including reproduction and distribution, or selling or licensing copies, or posting to personal, institutional or third party websites are prohibited.

In most cases authors are permitted to post their version of the article (e.g. in Word or Tex form) to their personal website or institutional repository. Authors requiring further information regarding Elsevier's archiving and manuscript policies are encouraged to visit:

http://www.elsevier.com/copyright

Author's personal copy

Annals of Physics 327 (2012) 671–704

Contents lists available at SciVerse ScienceDirect

Annals of Physics

journal homepage: www.elsevier.com/locate/aop

Analytical description of the coherent state model for near vibrational and well deformed nuclei

A.A. Raduta [a,b,*], R. Budaca [a], Amand Faessler [c]

[a] Department of Theoretical Physics, Institute of Physics and Nuclear Engineering, PO Box MG6, Bucharest 077125, Romania

[b] Academy of Romanian Scientists, 54 Splaiul Independentei, Bucharest 050094, Romania

[c] Institüt für Theoretishe Physik der Universität Tübingen, Auf der Morgenstelle 14, D-72076 Tübingen, Germany

ARTICLE INFO

Article history:
Received 12 July 2011
Accepted 21 October 2011
Available online 26 October 2011

Keywords:
Coherent state model
Rotational band
Phase transition
Critical point
Electric quadrupole transition probability
Excitation energy

ABSTRACT

Analytical formulas for the excitation energies as well as for the electric quadrupole reduced transition probabilities in the ground, beta and gamma bands were derived within the coherent state model for the near vibrational and well deformed nuclei. Numerical calculations were performed for 42 nuclei exhibiting various symmetries and therefore with specific properties. Comparison of the calculation results with the corresponding experimental data shows a good agreement. The parameters involved in the proposed model satisfy evident regularities being interpolated by smooth curves. Few of them, which fall out of the curves, are interpreted as signatures for a critical point in a specific phase transition. This is actually supported also by the figures showing the excitation energy dependence on the angular momentum. The formulas provided for energies and $B(E2)$ values are very simple, being written in a compact form, and therefore easy to be handled to explain the new experimental data.

© 2011 Elsevier Inc. All rights reserved.

1. Introduction

Since the liquid drop model was developed [1], the quadrupole shape coordinates were widely used by both phenomenological and microscopic formalisms to describe the basic properties of nuclear systems. Based on these coordinates, one defines quadrupole boson operators in terms of which model Hamiltonians and transition operators are defined. Since the original spherical harmonic liquid drop

* Corresponding author at: Department of Theoretical Physics, Institute of Physics and Nuclear Engineering, PO Box MG6, Bucharest 077125, Romania. Tel.: +40 212113301.
E-mail address: raduta@ifin.nipne.ro (A.A. Raduta).

0003-4916/$ – see front matter © 2011 Elsevier Inc. All rights reserved.
doi:10.1016/j.aop.2011.10.004

Author's personal copy

model was able to describe only a small amount of data for spherical nuclei, several improvements have been added. Thus, the Bohr–Mottelson model was generalized by Faessler and Greiner [2] in order to describe the small oscillations around a deformed shape which results in obtaining a flexible model, called the Vibration Rotation Model (VRM), suitable for the description of deformed nuclei. Later on [3], this picture was extended by including anharmonicities as low order invariant polynomials in the quadrupole coordinates. With a suitable choice of the parameters involved in the model Hamiltonian, the equipotential energy surface may exhibit several types of minima [4] like spherical, deformed prolate, deformed oblate, deformed triaxial, etc. To each equilibrium shape, specific properties for excitation energies and electromagnetic transition probabilities show up. Due to this reason, one customarily says that static values of intrinsic coordinates determine a phase for the nuclear system. A weak point of the boson description with a complex anharmonic Hamiltonian consists of the large number of the structure parameters which are to be fitted. A much smaller number of parameters is used by the coherent state model (CSM) [5] which uses a restricted collective space generated through angular momentum projection by three deformed orthogonal functions of coherent type. The model is able to describe in a realistic fashion transitional and well deformed nuclei of various shapes including states of high and very high angular momentum. Various extensions to include other degrees of freedom like isospin [6], single particle [7] or octupole degrees [8] of freedom have been formulated [9].

It has been noticed that a given nuclear phase may be associated to a certain symmetry. Hence, its properties may be described with the help of the irreducible representation of the respective symmetry group. Thus, the gamma unstable nuclei can be described by the $O(6)$ symmetry [10], the gamma triaxial nuclei by the rigid triaxial rotor $D2$ symmetry [11], the symmetric rotor by the $SU(3)$ symmetry and the spherical vibrator by the $U(5)$ symmetry. Thus, even in the 50s, the symmetry properties have been greatly appreciated. However, a big push forward was brought by the interacting boson approximation (IBA) [12,13], which succeeded to describe the basic properties of a large number of nuclei in terms of the symmetries associated to the system of quadrupole (d) and monopole (s) bosons which generate a $U(6)$ algebra. The three limiting symmetries $U(5)$, $O(6)$ and $SU(3)$ mentioned above, are dynamic symmetries for $U(6)$. Moreover, for each of these symmetries, a specific group reduction chain provides the quantum numbers characterizing the states, which are suitable for a certain region of nuclei. Besides the virtue of unifying the group theoretical descriptions of nuclei exhibiting different symmetries, the procedure defines very simple reference pictures for the limiting cases. For nuclei lying close to the region characterized by a certain symmetry, the perturbative corrections are to be included. In Refs. [14,15], it was shown that the critical points of some transitions correspond themselves to certain symmetries which may be described by the solutions of specific differential equations.

Many publications developing the mentioned formalisms as well advancing new approaches have been accumulated over time. To mention them would take too much space and moreover, one meets the risk of omitting involuntary some valuable contribution. Due to these reasons, we shall mention only those papers which are related to the present work.

The present paper is devoted to a systematic study of the CSM approach. In performing the present investigation, we have been stimulated by our previous publication [16], where the ground band energies for states of angular momentum going up to high values (36) and for a large number of nuclei (44), have been described with very high accuracy with very simple and compact formulas. Thus, in a way, this work is a natural extension of the procedure of the quoted paper to the excited bands. The exact and complex formulas for the matrix elements of the model Hamiltonian as well as of the $E2$ transition operator have been expanded in power series of a deformation variable $x\,(=d^2$ where d is a real parameter which simulates the nuclear deformation) for small deformation and in power series of $1/x$ when the nuclear deformation is large. As a result, analytical compact formulas are obtained for both excitation energies and quadrupole electric transition probabilities. These formulas are positively tested for a large number of nuclei.

The above mentioned project was achieved according to the following plan. The basic ideas of the CSM approach are shortly reviewed in Section 2. The near vibrational regime is described in Section 3, while the asymptotic expansion for large deformations is given in Section 4. Numerical applications are presented in Section 5 and the final conclusions are summarized in Section 6.

Author's personal copy

2. The coherent state model for three interacting bands

The model proposed in Ref. [5] is known under the name of CSM (coherent state model) and aims at describing in a realistic fashion, the lowest three rotational bands, ground, beta and gamma. Here we describe briefly the basic ingredients. First, one builds up a collective boson space being guided by the experimental picture. Thus, each band is generated by projecting the angular momentum from three orthogonal deformed states which modeled the ground, beta and gamma bands respectively, in the intrinsic frame of reference. The deformed ground band state is an axially deformed coherent state ψ_g, while the other two intrinsic states are orthogonal polynomial excitations of the ground band model function. These excitations were chosen such that they are mutually orthogonal both before and after angular momentum projection. All three states are dependent on a real parameter d which simulates the nuclear deformation. In the limit $d \to 0$, the projected states must go to the first three highest seniority states of the boson multiplets while in the asymptotic region, i.e. large value for d, the states written in the intrinsic frame of reference have expressions similar to those associated to the liquid drop model, in the strong coupling regime. By this requirement, we assure that the model states have a behavior which is consistent with the so called Sheline–Sakai scheme [17,18] which makes a continuous link between the vibrational and rotational spectra. These properties are satisfied by the following three sets of projected states:

$$\phi^g_{JM}(d) = N^g_J P^J_{M0}\psi_g, \quad \psi_g = \exp\left[d(b^\dagger_0 - b_0)\right]|0\rangle, \tag{2.1}$$

$$\phi^\beta_{JM}(d) = N^\beta_J P^J_{M0}\Omega^\dagger_\beta\psi_g, \quad \Omega^\dagger_\beta = \left(b^\dagger b^\dagger b^\dagger\right)_0 + \frac{3d}{\sqrt{14}}\left(b^\dagger b^\dagger\right)_0 - \frac{d^3}{\sqrt{70}}, \tag{2.2}$$

$$\phi^\gamma_{JM}(d) = N^\gamma_J P^J_{M2}\Omega^\dagger_{\gamma,2}\psi_g, \quad \Omega^\dagger_{\gamma,m} = \left(b^\dagger b^\dagger\right)_{2,m} + d\sqrt{\frac{2}{7}}b^\dagger_m. \tag{2.3}$$

Within the restricted space just defined, one constructs an effective Hamiltonian by requiring a maximal decoupling, i.e. the off diagonal matrix elements are equal or close to zero. Ideal would be to have a diagonal Hamiltonian but this is not possible due to the gamma band. However, one solution is given by the six order quadrupole boson Hamiltonian:

$$H^{(2)} = A_1(22\hat{N} + 5\Omega^\dagger_{\beta'}\Omega_{\beta'}) + A_2\hat{J}^2 + A_3\Omega^\dagger_\beta\Omega_\beta, \quad \Omega^\dagger_{\beta'} = \left(b^\dagger b^\dagger\right)_0 + \frac{d^2}{\sqrt{5}}, \tag{2.4}$$

where $\hat{N}$ denotes the quadrupole boson number operator:

$$\hat{N} = \sum_{\mu=-2}^{2} b^\dagger_\mu b_\mu. \tag{2.5}$$

Indeed, $H^{(2)}$ has the property that its matrix elements between a beta band state and a ground band or a gamma band state are vanishing.

The interaction of the β-band with the rest of the boson space might be simulated by some additional terms in the model Hamiltonian, which do not affect the decoupling feature of the band:

$$\Delta H = A_4(\Omega^\dagger_\beta\Omega^2_{\beta'} + h.\,c.) + A_5\Omega^{\dagger 2}_{\beta'}\Omega^2_{\beta'}. \tag{2.6}$$

Thus, the total Hamiltonian used by CSM for describing the ground, beta and gamma bands has the form:

$$H = H^{(2)} + \Delta H. \tag{2.7}$$

The matrix elements of H between the states presented above are expressed in terms of the basic overlap integral $I^{(0)}_J$ and its k-th derivatives, defined by

Author's personal copy

$$I_J^{(0)}(d^2) = \int_0^1 P_J(y) e^{d^2 P_2(y)} dy, \qquad I_J^{(k)}(x) = \frac{d^k I_J^{(0)}}{dx^k}, \quad x = d^2, \tag{2.8}$$

where P_J denotes the Legendre polynomial of rank J.

3. The vibrational and near vibrational regimes

3.1. Energies

As already mentioned, in Refs. [19–21], it was proved that the projected states go to the first three highest seniority states respectively, when the parameter d goes to zero. For an easier writing, let us denote:

$$\begin{aligned} &\varphi_{JM}^{i,v} = \lim_{d\to 0} \varphi_{JM}^{i}(d), \\ &H^v = \lim_{d\to 0} H. \end{aligned} \tag{3.1}$$

According to Refs. [19–21], the vibrational limits for the projected states are

$$\begin{aligned} \varphi_{JM}^{g,v} &= \left|\frac{J}{2}, \frac{J}{2}, 0, J, M\right\rangle, \\ \varphi_{JM}^{\gamma,v} &= \left|\left[\frac{J+3}{2}\right], \left[\frac{J+3}{2}\right], 0, J, M\right\rangle, [\cdots]\text{-integer part}, \\ \varphi_{JM}^{\beta,v} &= \left[1 - \frac{6}{7}\frac{J(2J+3)}{(J+7)(3J+10)}\right]^{\frac{1}{2}} \left|\frac{J}{2}+3, \frac{J}{2}+3, 1, J, M\right\rangle \\ &\quad + \left[\frac{6}{7}\frac{J(2J+3)}{(J+7)(3J+10)}\right]^{\frac{1}{2}} \left|\frac{J}{2}+3, \frac{J}{2}+1, 0, J, M\right\rangle \\ &\equiv \varphi_{JM}^{\beta v,1} + \varphi_{JM}^{\beta v,2} \end{aligned} \tag{3.2}$$

where, the standard notations for the states $|N, v, \alpha, J, M\rangle$, labeled by the number of bosons (N), seniority (v), missing quantum number (α), angular momentum (J) and its projection on z axis (M), are used. These quantum numbers, except α, are given by the Casimir operators of the groups in the chain $SU(5) \supset R(5) \supset R(3) \supset R(2)$. A complete description of these states may be found in Refs. [22,23]. The vibrational limits are related by the following equations:

$$\begin{aligned} \varphi_{JM}^{\beta v,1} &= \left[\frac{3}{5}(3J+10)\right]^{-\frac{1}{2}} (b^\dagger b^\dagger b^\dagger)_0 \varphi_{JM}^{g,v}, \\ \varphi_{JM}^{\beta v,2} &= \left[\frac{15}{7}\frac{J(2J+3)}{(J+7)^2(3J+10)}\right]^{\frac{1}{2}} (b^\dagger b^\dagger)_0 \varphi_{JM}^{\gamma,v}. \end{aligned} \tag{3.3}$$

The vibrational limit for the band energies are

$$\begin{aligned} E_J^{g,v} &= 11A_1 J + A_2 J(J+1), \\ E_J^{\gamma,v} &= 22A_1\left[\frac{J+3}{2}\right] + A_2 J(J+1), \\ E_J^{\beta,v} &= A_1\left[11(J+6) + \frac{12}{7}\frac{J(2J+3)}{3J+10}\right] + A_2 J(J+1) + \frac{3}{5}A_3(3J+10) \end{aligned} \tag{3.4}$$

where $[\cdots]$ denotes the integer part. Since the matrix elements of the model Hamiltonian between states of ground and gamma bands are vanishing in the vibrational limit, it results that the vibrational states are eigenstates of H in the restricted collective space. Moreover, one can prove that this is true

Author's personal copy

in the whole boson space for ground and gamma band states of any angular momentum. Concerning the beta band states, this property holds only for the $J = 0$ state. However, if one ignores the component $\varphi^{\beta v,2}_{JM}$ of the vibrational beta states, the remaining component, i.e. $\varphi^{\beta v,1}_{JM}$, is an eigenstate of the vibrational Hamiltonian:

$$H^v\varphi^{\beta v,1}_{JM} = \left[11A_1(J+6) + A_2J(J+1) + \frac{3}{5}(3J+10)A_3\right]\varphi^{\beta v,1}_{JM}. \tag{3.5}$$

For small values of the deformation parameter, the exact energies can be expressed as a power series in d. As a result, the excitation energies of the three bands are written as compact formulas depending on powers of $J(J+1)$ which are easy to be handled in numerical calculations. As we have already mentioned the matrix elements of the model Hamiltonian between the angular momentum projected states can be written as a function of the overlap integral $I^{(0)}_J$ and its k-th derivatives, $I^{(k)}_J$. Taking into account the composition rule as well as the recurrence relations for the Legendre polynomial, one can prove that the basic integrals satisfy the differential equation:

$$\frac{d^2I^{(0)}_J}{dx^2} - \frac{x-3}{2x}\frac{dI^{(0)}_J}{dx} - \frac{2x^2+J(J+1)}{4x^2}I^{(0)}_J = 0, \quad (x = d^2). \tag{3.6}$$

The solution for this equation is

$$I^{(0)}_J(d^2) = \frac{(J!)^2}{\left(\frac{J}{2}\right)!(2J+1)!}(6d^2)^{\frac{J}{2}}e^{-\frac{d^2}{2}}\,{}_1F_1\left(\frac{1}{2}(J+1), J+\frac{3}{2}; \frac{3}{2}d^2\right), \tag{3.7}$$

where ${}_1F_1(a, b; z)$ is the hypergeometric function of the first kind. The excitation energies of the ground, beta and gamma bands are functions of the ratio $d^2\frac{I^{(1)}_J}{I^{(0)}_J}$ and its first three derivatives with respect to d^2. These quantities have the following vibrational limits:

$$\lim_{d\to 0}\left(d^2\frac{I^{(1)}_J}{I^{(0)}_J}\right)^{(k)} = \frac{1}{(2J+3)^k}\left[\frac{J}{2}(\delta_{k,0}+\delta_{k,1}) + 9\frac{(J+1)(J+2)}{2J+5}\left(\delta_{k,2} + 9\frac{\delta_{k,3}}{2J+7}\right)\right], \quad k = 0, 1, 2, 3. \tag{3.8}$$

These relations allow us to write down the Taylor expansion of $xI^{(1)}_J/I^{(0)}_J$ up to the third order in $x\,(= d^2)$:

$$x\frac{I^{(1)}_J}{I^{(0)}_J} = \frac{J}{2} + \frac{J}{2(2J+3)}x + \frac{9}{2}\frac{(J+1)(J+2)}{(2J+3)^2(2J+5)}x^2 + \frac{27}{2}\frac{(J+1)(J+2)}{(2J+3)^3(2J+5)(2J+7)}x^3. \tag{3.9}$$

Inserting the truncated power series of the $xI^{(1)}_J/I^{(0)}_J$, into the excitation energy expressions, one obtains [24]:

$$E^g_J = 22A_1\sum_{k=0}^{3}A^{(g)}_{J,k}x^k + A_2J(J+1) - \Delta E_J, \tag{3.10}$$

$$E^\gamma_J = 44A_1 + \frac{A_1}{\sum_{k=0}^{3}Q^{(\gamma,0)}_{J,k}x^k}\left[\sum_{k=0}^{3}\left(22R^{(\gamma,0)}_{J,k} + 5U^{(\gamma,0)}_{J,k}\right)x^k\right] + A_2J(J+1) + \Delta E_J, \quad J = \text{even}, \tag{3.11}$$

$$E^\gamma_J = 44A_1 + \frac{A_1}{\sum_{k=0}^{3}Q^{(\gamma,1)}_{J,k}x^k}\left[\sum_{k=0}^{3}\left(22R^{(\gamma,1)}_{J,k} + 5U^{(\gamma,1)}_{J,k}\right)x^k\right] + A_2J(J+1), \quad J = \text{odd}, \tag{3.12}$$

Author's personal copy

$$E_J^\beta = \frac{1}{\sum_{k=0}^{3} Q_{J,k}^{(\beta)} x^k}\left\{A_1\sum_{k=0}^{3}\left(22R_{J,k}^{(\beta)}+5U_{J,k}^{(\beta)}\right)x^k+\sum_{k=0}^{3}\left(A_3V_{J,k}^{(\beta)}+A_4dZ_{J,k}^{(\beta)}+A_5B_{J,k}^{(\beta)}\right)x^k\right\} + A_2J(J+1). \tag{3.13}$$

The expansion coefficients A, R, U, V, Z, B and the quantity ΔE are given in Appendix A.

3.2. Reduced probability for E2 transitions

CSM uses for the quadrupole transition operator the following expression:

$$Q_{2\mu} = q_h(b_\mu^\dagger + (-)^\mu b_{-\mu}) + q_{anh}((b^\dagger b^\dagger)_{2\mu} + (bb)_{2\mu}) \equiv Q_{2\mu}^h + Q_{2\mu}^{anh}. \tag{3.14}$$

The anharmonic term is the lowest order term in bosons which brings a non-vanishing contribution to the $E2$ transition between a state from the beta band and a state from the ground band.

Analytical expressions for transition probabilities are also possible. First we list the results for the limit of $d \to 0$ of the non-vanishing matrix elements of the terms involved in the transition operator.

The final results are [20,21]:

$$\lim_{d\to 0}\langle\varphi_J^g||Q_2^h||\varphi_{J'}^g\rangle = (1-\delta_{J,J'})\left[\frac{2}{3}\frac{(J+J'+3)(J+J'+1)}{J+J'}\right]^{1/2} C^{J\,2\,J'}_{0\,0\,0}q_h,$$

$$\lim_{d\to 0}\langle\varphi_J^\beta||Q_2^h||\varphi_{J'}^\beta\rangle = (1-\delta_{J,J'})\left[\frac{2}{3}\frac{(J+J'+1)(J+J'+3)(3(J+J')+26)}{(J+J')(3(J+J')+14)}\right]^{1/2} C^{J\,2\,J'}_{0\,0\,0}q_h,$$

$$\lim_{d\to 0}\langle\varphi_J^\gamma||Q_2^h||\varphi_J^g\rangle = 2\left[\frac{(J+1)(2J+3)}{3(J-1)(J+2)}\right]^{1/2} C^{J\,2\,J}_{2\,-2\,0}q_h, \quad J=\text{even},$$

$$\lim_{d\to 0}\langle\varphi_J^\gamma||Q_2^h||\varphi_{J+1}^g\rangle = -\left[\frac{6(J+1)(J+2)^2(2J+3)}{J(2J+1)(2J^2+5J+11)}\right]^{1/2} C^{J\,2\,J+1}_{2\,-2\,0}q_h, \quad J=\text{odd},$$

$$\lim_{d\to 0}\langle\varphi_J^\beta||Q_2^h||\varphi_{J+2}^\gamma\rangle = 2\left[\frac{6(2J+3)(2J+5)(2J+7)}{7(J+3)(J+4)(3J+10)}\right]^{1/2} C^{J\,2\,J+2}_{0\,2\,2}q_h,$$

$$\lim_{d\to 0}\langle\varphi_J^\beta||Q_2^h||\varphi_{J+1}^\gamma\rangle = -\left[\frac{108(J+2)(J+3)^2}{7(3J+10)(2J^2+9J+18)}\right]^{1/2} C^{J\,2\,J+1}_{0\,2\,2}q_h,$$

$$\lim_{d\to 0}\langle\varphi_J^\gamma||Q_2^h||\varphi_{J+2}^\gamma\rangle = \left[\frac{(J+1)(J+2)(2J+5)(2J+7)}{3(J-1)(J+3)(J+4)}\right]^{1/2} C^{J\,2\,J+2}_{2\,0\,2}q_h, \quad J=\text{even},$$

$$\lim_{d\to 0}\langle\varphi_J^\gamma||Q_2^h||\varphi_{J+2}^\gamma\rangle = \left[\frac{(J+3)(2J+3)(4J^3+18J^2+45J+23)^2}{3J(2J+1)(J+1)(2J^2+13J+29)(2J^2+5J+11)}\right]^{1/2} \times C^{J\,2\,J+2}_{2\,0\,2}q_h, \quad J=\text{odd},$$

$$\lim_{d\to 0}\langle\varphi_J^\gamma||Q_2^h||\varphi_{J+1}^\gamma\rangle = -\left[\frac{3(J+1)(J+2)^2(J+3)^2}{2(J-1)(2J+3)(2J^2+9J+18)}\right]^{1/2} C^{J\,2\,J+1}_{2\,0\,2}q_h, \quad J=\text{even},$$

$$\lim_{d\to 0}\langle\varphi_J^g||Q_2^{anh}||\varphi_{J-2}^\beta\rangle = \left[\frac{4(J-1)J^2}{(2J-1)(2J+1)(3J+4)}\right]^{1/2} C^{J\,2\,J-2}_{0\,0\,0}q_h. \tag{3.15}$$

Note that in the limit of large J, Alaga's rule [25] is valid even for the vibrational regime.

Author's personal copy

It is well known that the $B(E2)$ values are very sensitive to the small variation in both the wave functions and transition operator. Therefore we include in the expression of the matrix elements of the transition operator the first order Taylor expansion in terms of the deformation parameter d. Then the $B(E2)$ value characterizing a certain transition is obtained, in the Rose convention [26], by squaring the corresponding reduced matrix element.

Intraband transition matrix elements are

$$\langle\phi_J^g||Q_2||\phi_{J-2}^g\rangle = \sqrt{\frac{J}{2}}\,(q_h - q_{anh}d)\,, \tag{3.16}$$

$$\langle\phi_J^\beta||Q_2||\phi_{J-2}^\beta\rangle = \sqrt{\frac{J(3J+10)}{2(3J+4)}}\left[q_h - \frac{q_{anh}d(3J+4)}{3J+10}\right], \tag{3.17}$$

$$\langle\phi_{J+2}^\gamma||Q_2||\phi_J^\gamma\rangle = \sqrt{\frac{J(2J+7)}{2(2J+3)}}\left[q_h - \frac{q_{anh}d(2J-13)}{2J+7}\sqrt{\frac{2}{7}}\right], \quad J = \text{even}, \tag{3.18}$$

$$\langle\phi_J^\gamma||Q_2||\phi_{J-1}^\gamma\rangle = q_h d\sqrt{\frac{2(J-2)}{J(J-1)(2J+3)}}\left[8 - \frac{J-8}{2J-1}\right. \tag{3.19}$$

$$\left. + \frac{(J+2)(2J+3)}{(J+1)(2J+1)} + \frac{2(J-5)(J-1)(4J+3)}{(J+1)(2J-1)(2J+1)}\right], \quad J = \text{even}, \tag{3.20}$$

$$\langle\phi_{J+1}^\gamma||Q_2||\phi_J^\gamma\rangle = \sqrt{\frac{6(J+3)}{J(2J+3)}}\left[q_h - \frac{5q_{anh}d}{J+3}\sqrt{\frac{2}{7}}\right], \quad J = \text{even}, \tag{3.21}$$

$$\langle\phi_{J+2}^\gamma||Q_2||\phi_J^\gamma\rangle = \sqrt{\frac{(J-1)(J+3)(J+4)}{2(J+1)(J+2)}}\left[q_h - q_{anh}d\frac{J+6}{J+4}\sqrt{\frac{2}{7}}\right], \quad J = \text{odd}. \tag{3.22}$$

The interband transition matrix elements are

$$\langle\phi_J^g||Q_2||\phi_{J-2}^\beta\rangle = q_{anh}\sqrt{\frac{6J}{(3J+4)}}\left[1 - \frac{3(34J^2+34J-29)}{14(2J-1)(2J+3)(3J+4)}d^2\right], \tag{3.23}$$

$$\langle\phi_J^g||Q_2||\phi_J^\beta\rangle = -2q_{anh}d\sqrt{\frac{3J(J+1)}{(2J-1)(2J+3)(3J+10)}}, \tag{3.24}$$

$$\langle\phi_{J-2}^g||Q_2||\phi_J^\beta\rangle = q_{anh}d^2\frac{3(J-1)}{2J-1}\sqrt{\frac{6J}{(2J-3)(2J+1)(3J+10)}}, \tag{3.25}$$

$$\langle\phi_J^\gamma||Q_2||\phi_J^g\rangle = \sqrt{\frac{2(J+1)}{2J-1}} \times\left[q_h + \frac{2q_{anh}d(44J^4-210J^3-533J^2-15J+378)}{7(J-1)(J+1)(2J+3)^2}\sqrt{\frac{2}{7}}\right], \tag{3.26}$$

$$\langle\phi_J^\gamma||Q_2||\phi_{J-2}^g\rangle = \sqrt{(2J+3)}\left[q_{anh}\sqrt{\frac{2}{7}} + \frac{3q_h d}{(2J+3)(2J-1)}\right], \tag{3.27}$$

$$\langle\phi_J^\gamma||Q_2||\phi_{J+2}^g\rangle = \frac{6q_h d(J-1)}{(J+1)(2J+3)}\sqrt{\frac{J(J+2)(2J+5)}{(2J+1)(2J+3)}}, \tag{3.28}$$

Author's personal copy

$$\langle\phi^{\gamma}_{J-1}||Q_2||\phi^{g}_{J}\rangle = -\sqrt{\frac{(J-2)(2J+1)}{(J-1)(2J-1)}}\left[q_h + q_{anh}d\frac{(J+3)(J+4)}{(2J+1)(J+1)}\sqrt{\frac{2}{7}}\right], \tag{3.29}$$

$$\langle\phi^{\gamma}_{J+1}||Q_2||\phi^{g}_{J}\rangle = -\sqrt{3(J+3)}\left[q_{anh}\sqrt{\frac{2}{7}} + \frac{q_h d}{(2J+3)}\right], \tag{3.30}$$

$$\langle\phi^{\beta}_{J}||Q_2||\phi^{\gamma}_{J+2}\rangle = \sqrt{\frac{6(2J+5)(2J+7)}{7(2J+1)(3J+10)}}\left[q_h + q_{anh}d\frac{8J^2+42J+21}{(2J+3)(2J+7)}\sqrt{\frac{2}{7}}\right], \tag{3.31}$$

$$\begin{aligned}\langle\phi^{\beta}_{J}||Q_2||\phi^{\gamma}_{J}\rangle \;=\; & 4(J+5)\sqrt{\frac{3(J+1)}{7(2J-1)(3J+10)}} \\ & \times\left[q_{anh}\sqrt{\frac{2}{7}} + q_h d\frac{10J^2+13J-33}{2(J+1)(J+5)}\right],\end{aligned} \tag{3.32}$$

$$\langle\phi^{\beta}_{J+2}||Q_2||\phi^{\gamma}_{J}\rangle = q_{anh}d\sqrt{\frac{3J(J+2)}{(2J+3)(3J+16)}}\frac{8(5J^2+17J-27)}{7(J+1)(2J+3)}. \tag{3.33}$$

In the limit $d \to 0$, these expressions reproduce the m.e. corresponding to vibrational case (3.15), where some transitions are forbidden [20,27]. Taking the next leading order of the transition m.e. (see Appendix C), the mentioned selection rules are washed out.

4. Large deformation regime

One salient feature of CSM is the behavior of the projected states as function of the deformation parameter especially for the extreme limits of $d \to 0$ and large d. While in the vibrational limit these are just multiphonon states in the rotational regime, i.e. for asymptotic values for deformation parameter d, the wave functions of the ground, beta and gamma band states predicted by the liquid drop model [1] in the large deformation regime are nicely simulated. Indeed, as proved in Ref. [5], writing the projected states in the intrinsic reference frame and then considering a large deformation d, one obtains

$$\begin{aligned}\varphi^{i}_{JM} \;=\; & C_J\beta^{-1}e^{-(d-\frac{k\beta}{\sqrt{2}})^2}\left[\delta_{i,g}D^{J*}_{M0}(\Omega_0) + \delta_{i,\beta}\frac{4d^2}{9\sqrt{114}}D^{J*}_{M0}(\Omega_0)\right. \\ & \left. + \delta_{i,\gamma}\beta f_J k\gamma\left(D^{J*}_{M2}(\Omega_0) + (-)^J D^{J*}_{M,-2}(\Omega_0)\right)\right],\end{aligned} \tag{4.1}$$

where k is a constant defining the canonical transformation relating the quadrupole bosons and the quadrupole collective conjugate coordinates:

$$\alpha_\mu = \frac{1}{k\sqrt{2}}(b^{\dagger}_{\mu} + (-)^{\mu}b_{-\mu}), \qquad \pi_\mu = \frac{ik}{\sqrt{2}}((-)^{\mu}b^{\dagger}_{-\mu} - b_\mu), \tag{4.2}$$

while the constants C_J and f_J are

$$C_J = \frac{2}{3}\pi^{-\frac{1}{4}}k^{2/3}(2J+1)^{1/2}, \qquad f_J = -\sqrt{2}(8+(-)^{J+1})^{-1/2}. \tag{4.3}$$

It is worth noticing that the model Hamiltonian yields for the ground band similar excitation energies as the effective Hamiltonian

$$H_{eff} = 11A_1\hat{N} + A_2\hat{J}^2. \tag{4.4}$$

Averaging this Hamiltonian on a vibrational ground band state, one obtains a quadratic expression in N, the number of bosons in the considered state:

$$\langle H_{eff}\rangle = N(11A_1 + 2A_2 + 4A_2N). \tag{4.5}$$

Author's personal copy

In the asymptotic region for d, the average matrix element of H_{eff} is [19] proportional to $J(J+1)$:

$$\langle H_{eff}\rangle = J(J+1)\left(\frac{11A_1}{6d^2}+A_2\right). \tag{4.6}$$

For the intermediate situation for the deformation parameter d, we may use for energies either rational functions of d with the coefficients being functions of the angular momentum as given in the previous section, or asymptotic expansion for the matrix elements in powers of $1/x$. The later version was developed in Ref. [27]. Here we sketch the ideas and give the final results.

4.1. Energies

The asymptotic expressions for the matrix elements are obtained by considering the behavior of the overlap integral $I_J^{(0)}$ for large d. This is obtained by using the asymptotic expression for the hypergeometric function:

$$F(a,c;z) = \frac{\Gamma(c)}{\Gamma(a)}e^z z^{a-c}[1+\mathcal{O}(|z|^{-1})]. \tag{4.7}$$

One finds that the dominant term of the asymptotic form of $I_J^{(0)}$ is

$$I_J^{(0)} \sim \frac{e^x}{3x}. \tag{4.8}$$

This suggests as trial function for the quantity $I_J^{(0)}$ satisfying the differential equation (3.6), the following series:

$$I_J^{(0)} = e^x \sum_{n=1} A_n x^{-n}. \tag{4.9}$$

This series expansion together with the differential equation offer a recurrence relation for the series coefficients.

$$A_{n+1} = \frac{A_n}{6n}(2n+J)(2n-J-1). \tag{4.10}$$

Using the asymptotic form (4.8) as the limit condition, which infers $A_1 = \frac{1}{3}$, solution (4.9) is completely determined.

For big values of the deformation parameter, the series can be approximated by a truncation, such that one arrives at the following expression

$$x\frac{I_J^{(1)}}{I_J^{(0)}} = x - 1 - \frac{1}{3x} - \frac{5}{9x^2} - \frac{37}{27x^3} + \left(\frac{1}{6x}+\frac{5}{18x^2}+\frac{13}{18x^3}\right)J(J+1) - \frac{1}{54x^3}J^2(J+1)^2 + \mathcal{O}(x^{-4}). \tag{4.11}$$

This approximation can be substantially improved. Indeed, let us write the differential equation (3.6) in the form

$$x\left(x\frac{I_J^{(1)}}{I_J^{(0)}}\right)' + \left(x\frac{I_J^{(1)}}{I_J^{(0)}}\right)^2 - \frac{x-1}{2}\left(x\frac{I_J^{(1)}}{I_J^{(0)}}\right) - \frac{2x^2+J(J+1)}{4} = 0 \tag{4.12}$$

and replace the first term by the derivative of expression (4.11). Obviously, one obtains a quadratic equation for the quantity $xI_J^{(1)}/I_J^{(0)}$ whose positive solution is

$$x\frac{I_J^{(1)}}{I_J^{(0)}} = \frac{1}{2}\left[\frac{x-2}{2}+\sqrt{G_J}\right], \tag{4.13}$$

Author's personal copy

where

$$G_J = \frac{9}{4}x(x-2) + \left(J+\frac{1}{2}\right)^2 - \frac{4}{9x}\left(3+\frac{10}{x}+\frac{37}{x^2}\right) + \frac{2}{3x}\left(1+\frac{10}{3x}+\frac{13}{x^2}\right)J(J+1) - \frac{2J^2}{9x^3}(J+1)^2. \tag{4.14}$$

Note that the mixing m.e. between ground and γ states are negligible within the approximation of large deformation.

Using approximation (4.11), the energies of the β and γ bands can be written as follows:

$$E_J^\beta = \frac{1}{P_J^\beta}\left[A_1 S_J^\beta + A_3 F_J^\beta\right] + A_2 J(J+1), \tag{4.15}$$

$$E_J^\gamma = A_1 \frac{S_J^\gamma}{P_J^\gamma} + A_2 J(J+1). \tag{4.16}$$

The polynomials P, S, F, in $J(J+1)$, are given in Appendix B. To these equations, we add the equations determining the excitation energies in the ground band:

$$E_J^g = 11A_1\left[\frac{x-2}{2} + \sqrt{G}\right] + A_2 J(J+1). \tag{4.17}$$

In order to obtain a good agreement for β-band energies, the use of an additional term accompanied by the A_4 or the A_5 parameter is necessary for some cases. For these additional terms, the following asymptotic relations are used:

$$\langle \phi_{JM}^\beta | \Omega_\beta^\dagger \Omega_{\beta'}^2 + h.c. | \phi_{JM}^\beta \rangle = \frac{96d}{5\sqrt{70}}\left(\frac{x}{2} - \frac{T_J^{4,\beta}}{P_J^\beta}\right),$$

$$\langle \phi_{JM}^\beta | \Omega_{\beta'}^{\dagger 2} \Omega_{\beta'}^2 | \phi_{JM}^\beta \rangle = \frac{32}{875}\frac{T^{5,\beta}}{P_J^\beta}, \tag{4.18}$$

with the factors $T_J^{n,\beta}$, with $n = 4, 5$, and P_J^β defined in Appendix B.

4.2. Reduced probabilities for the E2 transitions

Taking the asymptotic limit of the exact m.e. of the quadrupole operator, one obtains a very simple formula for transition m.e. for large deformation case. The asymptotic expressions for the reduced m.e. of the harmonic quadrupole transition operator are [27]

$$\langle \phi_J^i || Q_2^h || \phi_{J'}^i \rangle = 2dq_h C_{K_i 0 K_i}^{J\,2\,J'}, \quad i = g, \beta, \gamma, K_i = -2\delta_{i\gamma}, \tag{4.19}$$

$$\langle \phi_J^\gamma || Q_2^h || \phi_{J'}^g \rangle = \sqrt{2} q_h C_{-2\,2\,0}^{J\,2\,J'}, \tag{4.20}$$

$$\langle \phi_J^\beta || Q_2^h || \phi_{J'}^\gamma \rangle = \frac{2}{3\sqrt{19}} q_h C_{0\,-2\,-2}^{J\,2\,J'}, \tag{4.21}$$

while the β and ground band states are connected by anharmonic part of $Q_{2\mu}$:

$$\langle \phi_J^\beta || Q_2^{anh} || \phi_{J'}^g \rangle = 2\sqrt{\frac{7}{19}} q_{anh} C_{0\,0\,0}^{J\,2\,J'}. \tag{4.22}$$

Note that in the asymptotic limit of the deformation parameter d, the projected functions are similar to that of the liquid drop model in the strong coupling regime. The Clebsch–Gordan factorization of the transition probabilities is known in the literature as Alaga's rule [25]. Thus, we may say that our description of the deformed nuclei is consistent with the Alaga's rule.

Author's personal copy

Table 1
The fitted parameters, d, A_1, A_2, A_3, A_4 and A_5 determining the ground, γ and β energies in the limit of small d, i.e. near vibrational regime, for 13 nuclei. Also we give the r.m.s. for the deviations of the calculated and experimental energies, denoted by χ, the total number of states in the considered three bands, the ratio $E_{4_1^+}/E_{2_1^+}$. In the first column are listed the nuclei and the reference from where the experimental data are taken.

Nucleus	$E_{4_1^+}/E_{2_1^+}$	d	A_1 [keV]	A_2 [keV]	A_3 [keV]	A_4 [keV]	A_5 [keV]	χ [keV]	Number of states
^{102}Pd [32]	2.293	1.45899	31.38296	8.58408	−48.05379	0	0	29.29906	11
^{126}Xe [33]	2.424	0.67610	16.98803	13.13610	−90.02417	−93.79735	0	37.42684	15
^{152}Gd [34]	2.194	1.51491	22.18661	2.18499	47.49858	77.67379	34.40286	33.04687	20
^{154}Dy [35]	2.233	1.53241	20.91108	3.36512	15.08504	51.90471	133.94467	44.59838	30
^{188}Os [36]	3.083	1.62319	12.52609	9.63624	0	−9.81638	0	27.74638	13
^{190}Os [37]	2.934	1.59990	11.27512	12.45678	0	0	163.08491	11.93490	14
^{192}Os [38]	2.820	1.61011	10.53492	13.70670	0	0	263.51135	40.11629	16
^{182}Pt [39]	2.705	1.69634	17.19040	3.67131	115.45535	99.68881	−11.03489	38.35839	24
^{186}Pt [40]	2.560	1.67744	17.34034	4.29899	109.10067	98.17453	−17.85114	35.31432	18
^{190}Pt [37]	2.492	0.74815	12.23722	11.16625	0	−3.45036	0	54.24460	12
^{194}Pt [41]	2.470	0.83137	11.49716	15.25325	−89.44485	−109.08323	0	27.23740	11
^{196}Pt [42]	2.465	0.95083	13.08631	15.24711	0	−11.04808	0	57.96742	13
^{186}Hg [40]	2.665	0.92388	20.30171	4.24561	−138.41747	−16.77953	1063.07400	53.10842	24

5. Numerical results

The analytical expressions for energies and transition probabilities presented in the previous sections were applied to 42 nuclei from which 18 are considered to be near vibrational while 24 are well deformed. The results are compared with the available data for both energies and reduced transition probabilities. Results are presented in a slightly different order than in the previous sections. Indeed, we divide this section into two parts, one devoted to energies and one to e.m. transitions. The reason is that we aim at pointing out the change in the spectrum structure and separately in the behavior of the transition probabilities when one passes from a near vibrational to a deformed regime.

5.1. Energies

Energies for near vibrational nuclei have been calculated with Eqs. (3.10)–(3.13). The parameters involved were calculated by a least squares procedure. The results are listed in Table 1. Therein, we also give the root mean square for the deviations of the calculated excitation energies from the corresponding experimental data, denoted by χ, the total number of states in the three bands, the ratio $E_{4_1^+}/E_{2_1^+}$. The mentioned ratio indicates how far we are from the vibrational limit which is 2. Another measure of this departure is of course the deformation parameter d. For nuclei close to a spherical shape, d is under-unity, while for a transitional nucleus, d may become larger than unity. Since the energies are power series of $x(=d^2)$, it is necessary to comment on the convergence of such series. A detailed study of this issue was presented in Ref. [16], where it was shown that the convergence radius of the series associated to the overlap integral $I_J^{(0)}$ is larger than unity. As a matter of fact, this property allows us to consider the nuclei from Table 1 with d larger than unity but smaller than the convergence radius found in Ref. [16] as belonging to the class of near vibrational isotopes.

Excitation energies in ground, beta and gamma bands are presented in Fig. 1 as function of angular momentum. The case of ^{152}Gd is included in Fig. 2 where the other even isotopes of Gd are presented. From Fig. 1, we notice that in ^{188,190,192}Os and ^{190,194,196}Pt, the three bands are well separated and evolve almost parallel with each other. All the mentioned nuclei are gamma unstable since the band gamma is less excited than the band beta. In ^{102}Pd and ^{126}Xe, the excited bands cross each other and they become gamma stable after the crossing point. In ^{182}Pt and ^{186}Pt, the excited bands are close to each other, this feature being associated with the $SU(3)$ symmetry. We remark that in ^{154}Dy, the excited bands and ground band are close to each other, which reflects the existence of a very flat potential in the β and very flat potential in the γ variable. A peculiar structure of the three bands

Author's personal copy

Table 2
The same as in Table 1 but for the Gd isotopic chain.

Nucleus	E_{4^+}/E_{2^+}	d	A_1 [keV]	A_2 [keV]	A_3 [keV]	χ [keV]	Number of states
^{154}Gd [35]	3.015	2.72583	18.68743	5.43251	−18.89754	38.51726	25
^{156}Gd [44]	3.239	3.08725	22.03879	3.84937	−15.81253	31.48198	35
^{158}Gd [45]	3.288	3.30765	21.45168	4.67653	−10.95906	10.07559	15
^{160}Gd [46]	3.302	3.31382	17.40521	5.69801	−1.72684	7.01074	19
^{162}Gd [47]	3.291	3.28976	15.19002	5.83600	2.43502	1.04853	11

Table 3
The same as in Table 1 but for other nuclei.

Nucleus	E_{4^+}/E_{2^+}	d	A_1 [keV]	A_2 [keV]	A_3 [keV]	χ [keV]	Number of states
^{228}Th [48,49]	3.235	3.20609	17.94631	1.58239	−7.03770	8.61377	21
^{230}Th [50]	3.273	3.21904	13.85032	2.82743	−9.72828	4.42896	20
^{232}Th [51]	3.284	3.37319	14.20081	2.53605	−7.87469	22.76356	40
^{232}U [51]	3.291	3.44137	15.73529	2.17430	−10.14916	5.28270	19
^{234}U [52]	3.296	3.66457	17.08527	1.73226	−9.05098	8.89688	25
^{236}U [53]	3.304	3.61576	17.51131	1.92143	−8.44386	2.28183	22
^{238}U [54]	3.303	3.74042	19.38859	1.60137	−10.11735	26.83668	44
^{238}Pu [54]	3.311	3.96825	18.78524	2.38340	−8.40586	1.03977	18
^{240}Pu [55]	3.309	4.06356	20.88751	1.83394	−11.17675	3.34091	19
^{242}Pu [56]	3.307	3.87399	20.15834	1.86784	−10.08071	2.90317	16
^{246}Cm [57]	3.314	4.17501	20.61062	2.28038	−7.00481	1.34909	9
^{248}Cm [58]	3.309	3.78738	19.18411	1.77579	−7.55677	4.11945	19

Table 4
The same as in Table 1 but for strongly deformed nuclei from the rare earth region.

Nucleus	E_{4^+}/E_{2^+}	d	A_1 [keV]	A_2 [keV]	A_3 [keV]	A_4 [keV]	χ [keV]	Number of states
^{150}Nd [58]	2.929	2.56790	19.49601	3.98450	−317.74302	−218.00288	21.85874	14
^{152}Sm [34]	3.009	2.69296	21.30931	4.03488	−20.22711	4.04777	47.24281	24
^{162}Dy [59]	3.294	3.09941	15.51332	6.30447	157.11712	113.15065	14.18735	28
^{164}Dy [60]	3.301	3.05374	13.15152	6.08637	0.0	0.0	4.60156	20
^{166}Er [61]	3.289	2.83539	13.80805	5.81240	89.40226	60.78307	5.90918	23
^{172}Yb [62]	3.305	3.69655	26.79492	4.83027	34.86006	36.41885	24.74324	20
^{174}Yb [63]	3.310	3.78841	29.85375	4.05312	−8.45732	4.17396	2.82653	17
^{176}Hf [64]	3.284	3.20357	25.26813	4.06412	33.53111	37.14456	28.12626	22
^{182}W [39]	3.291	3.20632	21.88739	7.37645	−125.28004	−81.67164	9.13062	15
^{186}W [40]	3.234	2.58620	12.34463	11.44538	−79.27311	−56.40554	15.05515	18
^{178}Os [65]	3.022	2.45573	16.62605	5.68882	−189.91058	−125.86003	37.91601	16
^{186}Os [40]	3.165	2.37861	13.52361	10.41550	121.91976	91.28338	32.58668	25

is seen for ^{186}Hg where the beta band crosses the ground band becoming yrast state from $J = 4$. As shown in Fig. 2, ^{152}Gd is a gamma stable nucleus. The results concerning the fitted parameters for the well deformed nuclei are given in Tables 2–4. Results for Gd isotopes are given separately in Table 2 and Fig. 2. Except ^{154}Gd, which seems to be the critical nucleus in the phase transition from $SU(5)$ to $SU(3)$ symmetry [28], all isotopes from Table 2 are characterized by values of d close to the rotational limit which is 3.3. From Fig. 2, one sees that the first three isotopes exhibit the features of a gamma stable nucleus while the heaviest two isotopes are gamma unstable nuclei. In ^{158}Gd, the excited bands having the states of even angular momentum degenerate which results in exhibiting an $SU(3)$ symmetry. For high odd angular momenta in gamma bands of ^{154}Gd and ^{156}Gd, the moment of inertia becomes different from that of even angular momentum states. This is caused by the series truncation, which does not assure the expansion convergence in this particular region of J. Fitted parameters for some transuranic nuclei are given in Table 3, while the calculated excitation energies are compared with the available corresponding data in Fig. 3. Except for ^{228,230}Th, which exhibit a triaxial shape [29], the listed nuclei have a ratio $E_{4_1^+}/E_{2_1^+}$ close to the rotational limit. From

Author's personal copy

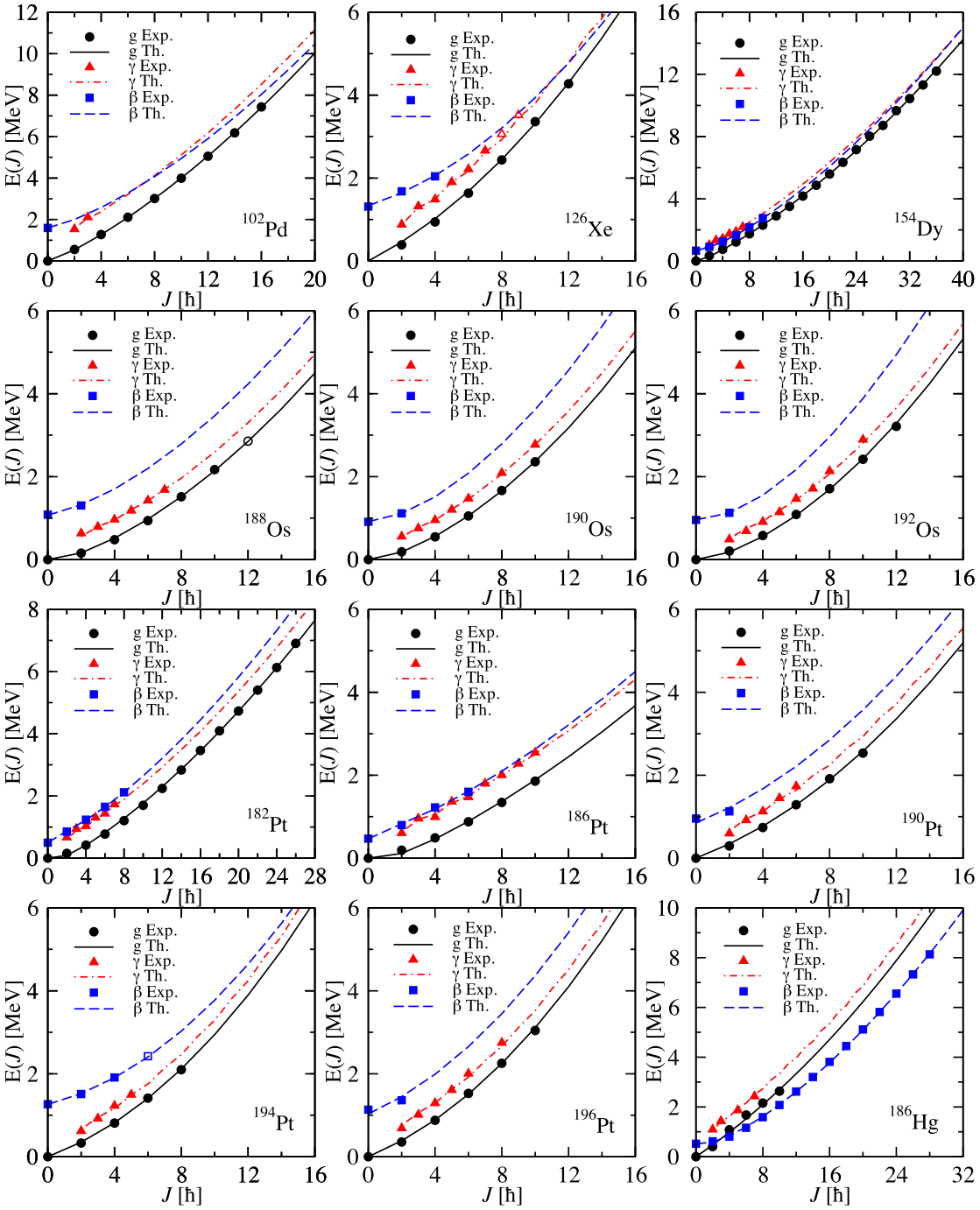

Fig. 1. Energy spectra of ground, γ and β bands described by means of vibrational formulas for nuclei belonging to different nuclear phases. Open symbols denote uncertain or with possible band assignment experimental points, which were not taken into account in the fitting procedure. Experimental data are taken from [32,33,35–42].

Table 3, one remarks the high accuracy for the theoretical description. Except for ^{228}Th, ^{232}U and ^{240}Pu, where the two excited bands are only slightly split apart, for other nuclei the excited states relative position reclaim on ideal $SU(3)$ symmetry. In Table 4, the fitted parameters for some deformed rare earth nuclei are presented. The energies ratio of the ground band states 4^+ and 2^+ ranges from 2.9 to 3.3. The lowest values 2.929, 3.009, 3.022 suggest that the nuclei to which they are assigned ^{150}Nd, ^{152}Sm and ^{178}Os satisfy the $X(5)$ symmetry. Four nuclei, ^{176}Hf, ^{182,186}W and ^{186}Os, have the signature of triaxial nuclei. The remaining nuclei have the above mentioned ratio close to 3.3, i.e. they belong to the rotational behaving nuclei. The plots from Fig. 4 show that for some nuclei like ^{152}Sm, ^{172}Yb and ^{186}W, the excited bands do not intersect each other. In ^{162}Dy, the intersection is associated to

Author's personal copy

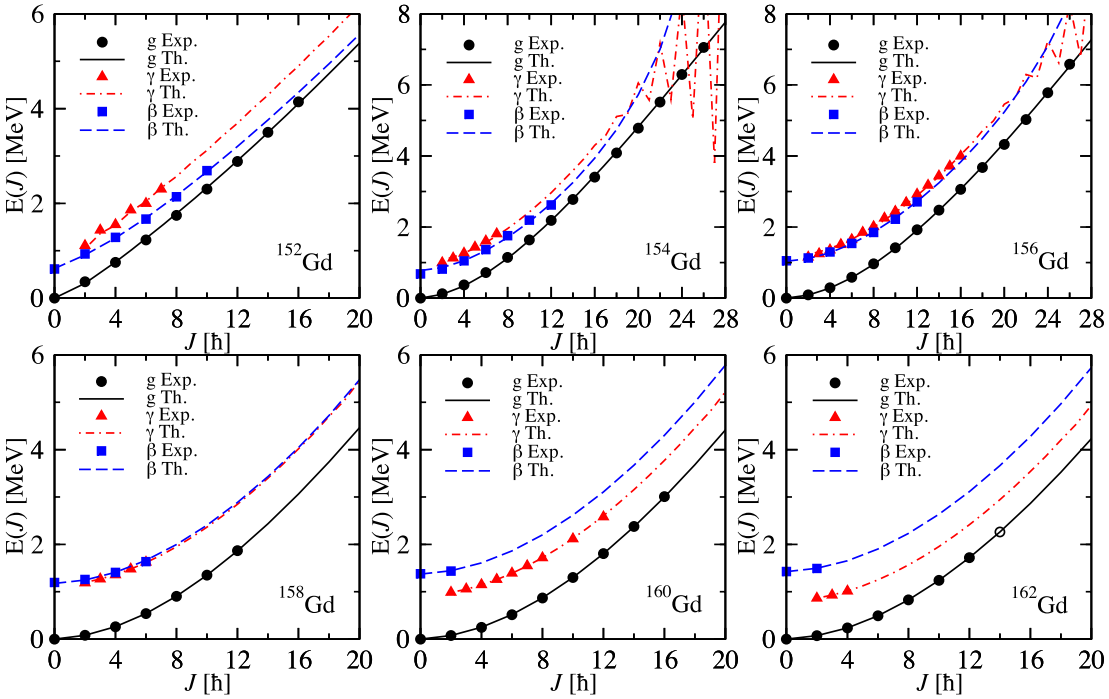

Fig. 2. The isotopic chain of Gd. First nucleus is treated like a near vibrational one, later ones are deformed nuclei described by means of asymptotic regime formulas with 4 parameters. Open symbols denote uncertain or with possible band assignment experimental points, which were not taken into account in the fitting procedure. Experimental data are taken from [34,35, 44–47].

the transition from the gamma unstable to the gamma stable behavior, while in ^{150}Nd the transition is, by contrary, from gamma stable to gamma unstable regime. For describing the complex structure of the three bands, the five parameters formulas are used. Exception is for ^{164}Dy where the set of three parameters formulas is used. The reduced number of the necessary parameters is explained by the fact that here the beta band is missing. Now we would like to comment on the change of parameters when we pass from one nucleus to another. This is done by plotting the deformation parameter as function of the nuclear deformation β_2, Fig. 5, and the structure coefficients as functions of $A + (N - Z)/2$, in Figs. 6–9. The atomic mass number was corrected by the third component of the isospin in order to infer also the result dependence on Z. In Fig. 5, it is shown that the three groups of nuclei, near vibrational, transuranic and rare earth deformed nuclei are spread around three distinct straight lines. The lines corresponding to the two groups of well deformed nuclei are almost parallel with each other. The line corresponding to the near vibrational nuclei has a smaller slope than the other two lines. The linear dependence of d on the quadrupole nuclear deformation β_2 has been studied analytically, in a different context, in Ref. [30]. The structure coefficient A_1 depends on $A + (N - Z)/2$ according to what is shown in Fig. 6. Again the three groups of nuclei satisfy distinct dependence law. While the transuranic and near vibrational nuclei lie on curves described by fourth order polynomials respectively, the deformed rare earth nuclei belong to a fifth order polynomial curve. Four rare earth nuclei fall apart from the interpolating curve. These are ^{164}Dy, ^{166}Er, ^{172}Yb and ^{174}Yb. The parameters A_2 yielded by the fitting procedure are interpolated by a sixth order polynomial. Note that the transuranic and the most deformed rare earth nuclei are concentrated around the two minima reflecting a large moment of inertia for a large deformation regime. Below the first minimum, five near vibrational nuclei are placed. These nuclei have a small nuclear deformation and therefore the parameter A_1 is decisive in determining the excitation energies in the three bands. An interesting dependence on $A+(N-Z)/2$ is shown in Fig. 8 for the structure coefficient A_3. Indeed, in that case, the points corresponding to the deformed rare earth nuclei cannot be interpolated by a single curve but by two parabolas. Three nuclei deviate substantially from the upper parabola. These are ^{162}Dy, ^{166}Er and ^{174}Yb. We remember that the band beta is decoupled from the ground and gamma bands. The coupling of this band to the upper bands is simulated by three boson terms having the coefficients A_3, A_4 and A_5. For the well deformed nuclei, only one term is sufficient in order to obtain a good description for

Author's personal copy

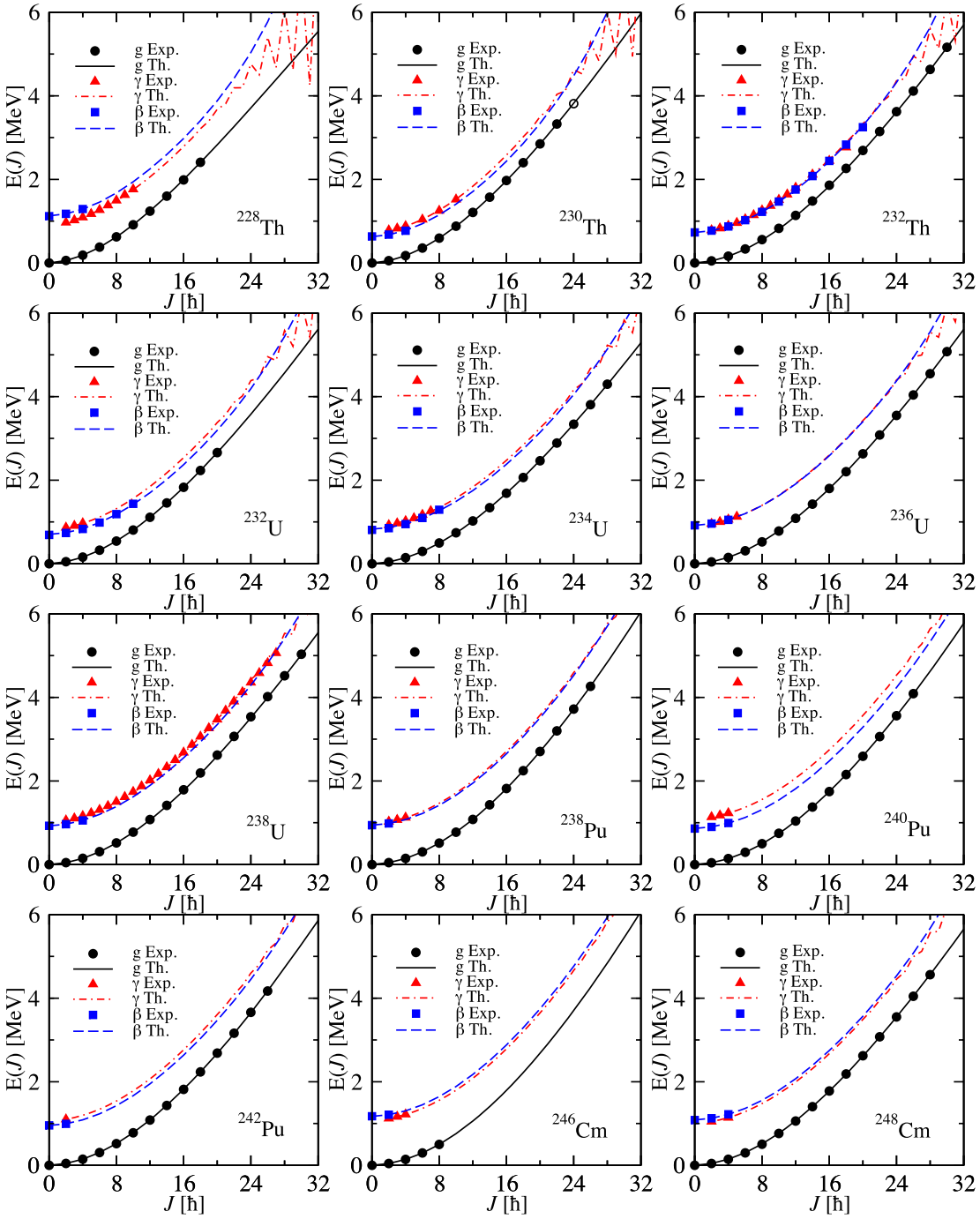

Fig. 3. Energy spectra of ground, γ and β bands described by means of asymptotic formulas with 4 parameters for $SU(3)$ nuclei from transuranic region. ^{228}Th and ^{230}Th are possible candidates for triaxial nuclei. Open symbols denote uncertain or with possible band assignment experimental points, which were not taken into account in the fitting procedure. Experimental data are taken form [48–57].

excitation energies in the beta band. This is the term multiplied by A_3. However, there are some nuclei where two terms responsible for this band excitations are necessary, A_3 and A_4, and for few nuclei (5) all three are necessary. We considered all nuclei where A_4 term was involved and plotted, in Fig. 9, the ratio A_3/A_4. From there it is seen that this ratio is close to unity. In this plot, we did not consider the case of ^{186}Hg where this rule is drastically violated due to the abnormal behavior of A_5. The points of this plot are interpolated with a straight line. Large deviation from this line is noticed for ^{152}Sm and ^{174}Yb. The first nucleus plays the role of a critical nucleus in a phase transition from $SU(5)$ to $SU(3)$ symmetry exhibiting $X(5)$ properties. The second nucleus seems to be the critical nucleus of a phase transition from a gamma stable to a gamma unstable nucleus, as suggested by Fig. 4. Actually,

Author's personal copy

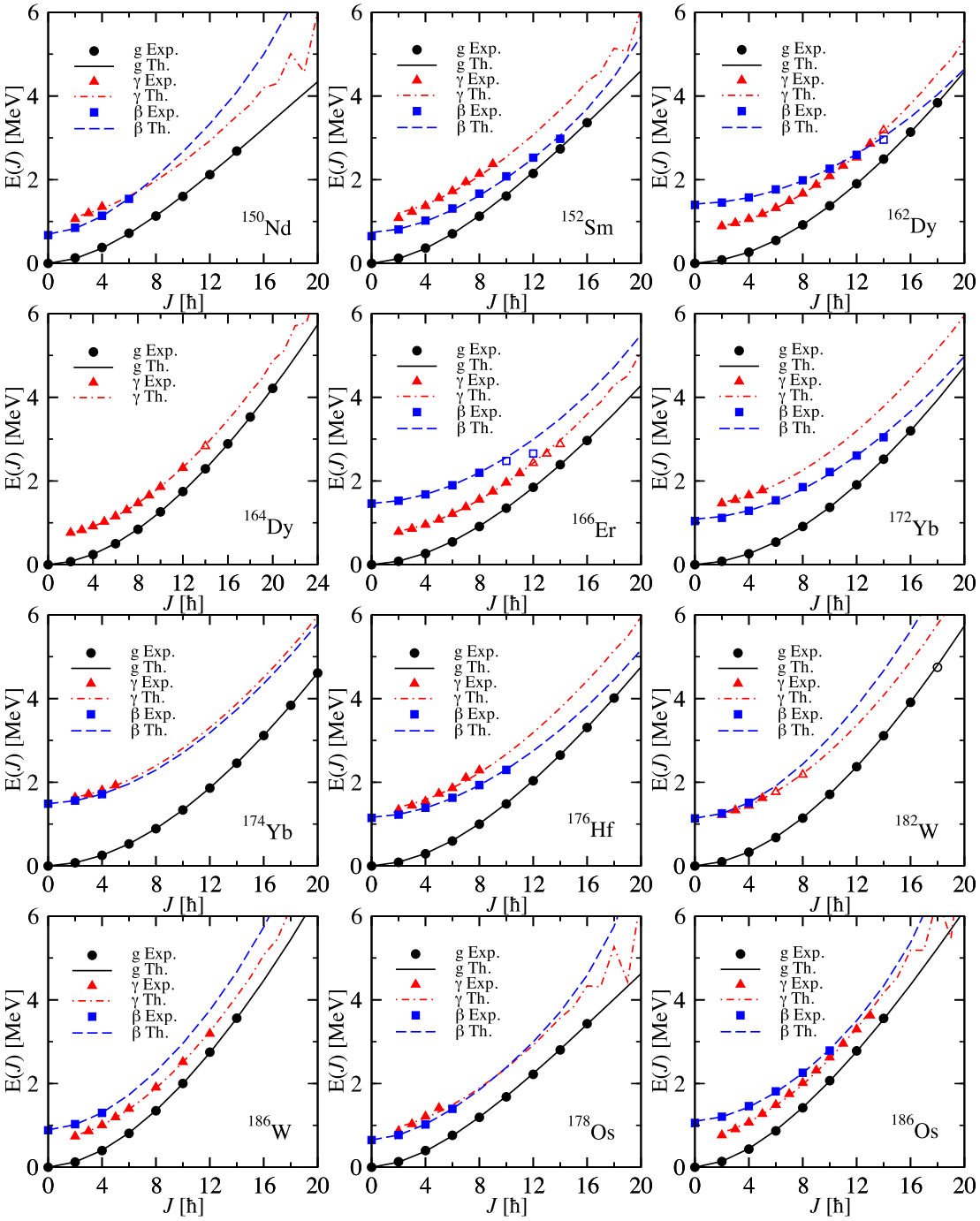

Fig. 4. Energy spectra of ground, γ and β bands described by means of asymptotic formulas with 5 parameters for strongly deformed nuclei from the rare earth region. Open symbols denote uncertain experimental points or probable band assignment, and were not taken into account in the fitting procedure. Experimental data are taken from [39,40,58,34,59–65].

this assertion is confirmed also by the graphs for A_1 and A_3, where the interpolating curves have a finite discontinuity. A large deviation from the smooth interpolating curve is seen for the parameter A_3 characterizing the isotope ^{162}Dy. In the graph associated with A_1, the discontinuity is met in ^{164}Dy and not ^{162}Dy. This is caused by the fact that the phase transition in this case is a slow process and not a sharp one. Coming back to Fig. 4, we note that the excited bands intersect each other. This might be a sign that this nucleus, ^{162}Dy, is critical for a phase transition from gamma unstable to a gamma stable regime. A similar situation is found for ^{166}Er which is also reflected in the discontinuities of the structure coefficients A_1 and A_3. In contradistinction to our interpretation in Ref. [31], the isotopes ^{166}Er and ^{164}Dy are considered critical points for the transition from triaxial to axially symmetric

Author's personal copy

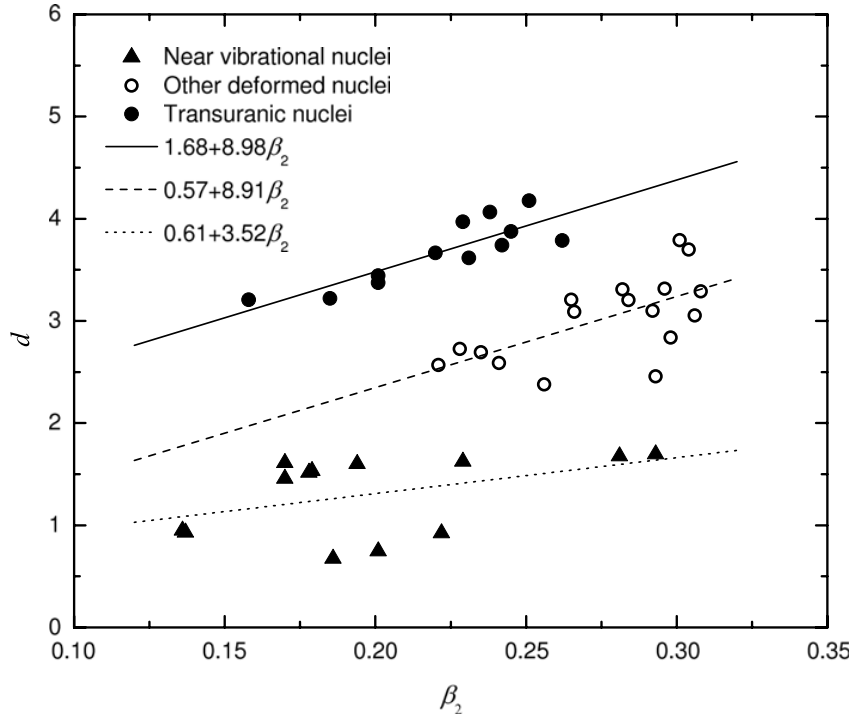

Fig. 5. The deformation parameter d as function of the nuclear deformation β_2 taken from Ref. [43].

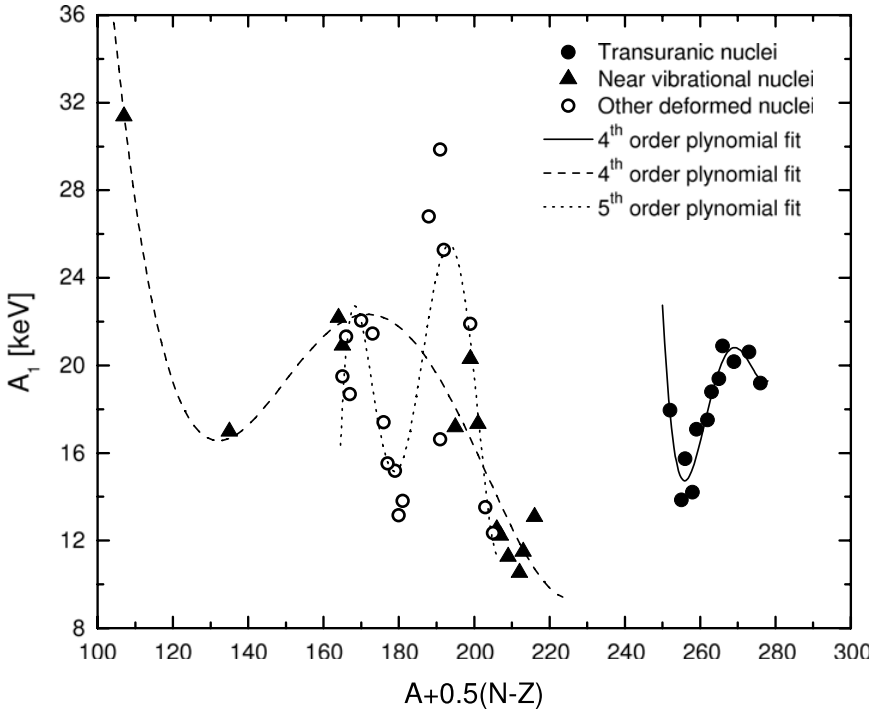

Fig. 6. The parameter A_1 as yielded by the fitting procedure as function of $A + (N - Z)/2$. The points corresponding to each group of nuclei were interpolated by a suitable polynomial.

shapes, exhibiting the so called Y(5) symmetry. In contrast to the results of Ref. [28], where the isotope ^{154}Gd is considered to be critical in the transition from the $SU(5)$ to the $SU(3)$ symmetry, here Fig. 8 shows a discontinuity in the A_3 behavior for ^{152}Gd. Indeed, this nucleus is symbolized by the third triangle from the left which stays apart from the rest of the Gd even isotopes represented by the second up to sixth half filled circles from the upper parabola. Note, however, that here ^{152}Gd is described by

Author's personal copy

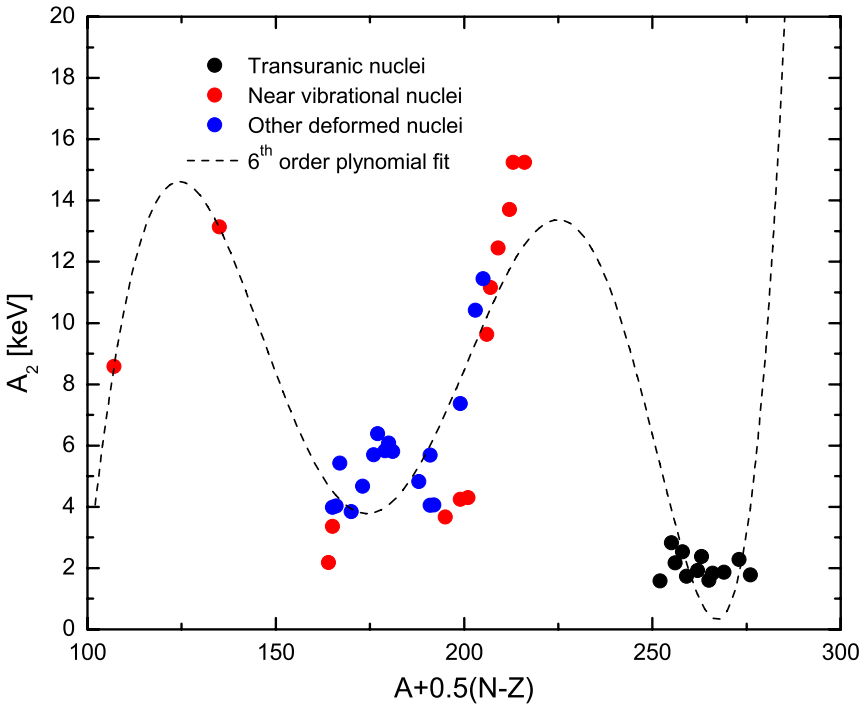

Fig. 7. The same as in Fig. 6, but for A_2.

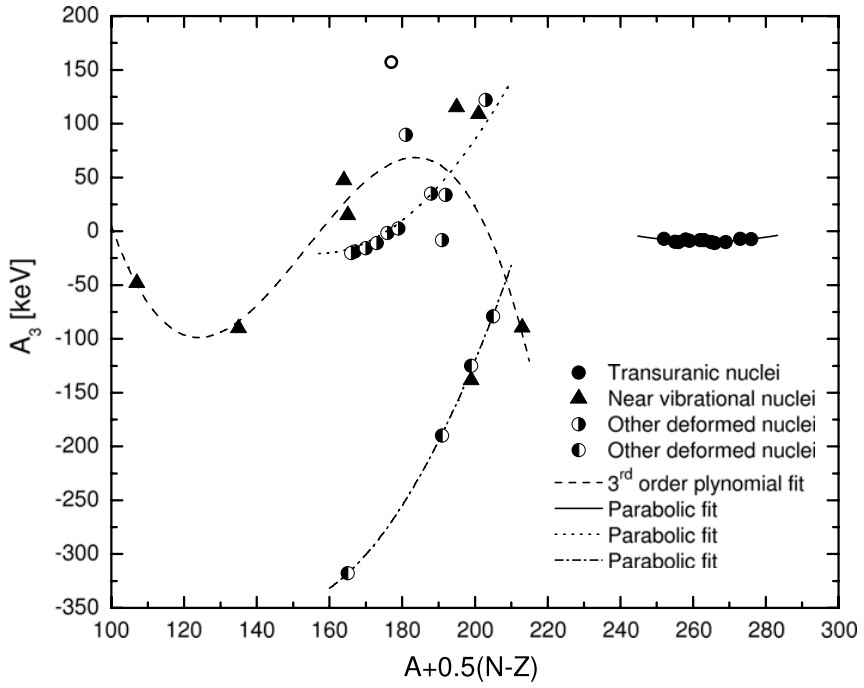

Fig. 8. The parameter A_3 as yielded by the fitting procedure as function of $A+(N-Z)/2$. There are four groups of nuclei, three of them having A_3 which could be interpolated by distinct parabolas and one with the corresponding A_3 parameters interpolated by a third order polynomial.

a different analytical formula from the rest of the isotopes and moreover, by using two additional fitting parameters. However, comparing the $B(E2)$ values associated to the transition $2_g^+ \rightarrow 0_g^+$ in the neighboring isotopes ^{152}Gd and ^{154}Gd, we notice a ratio larger than 2 in the favor of the second nucleus. Therefore it is more plausible to consider ^{154}Gd as a critical nucleus.

Concluding, except for a few nuclei which play the role of critical nuclei for some specific phase transitions, all structure coefficients show a smooth dependence on $A + (N - Z)/2$. The deformation

Author's personal copy

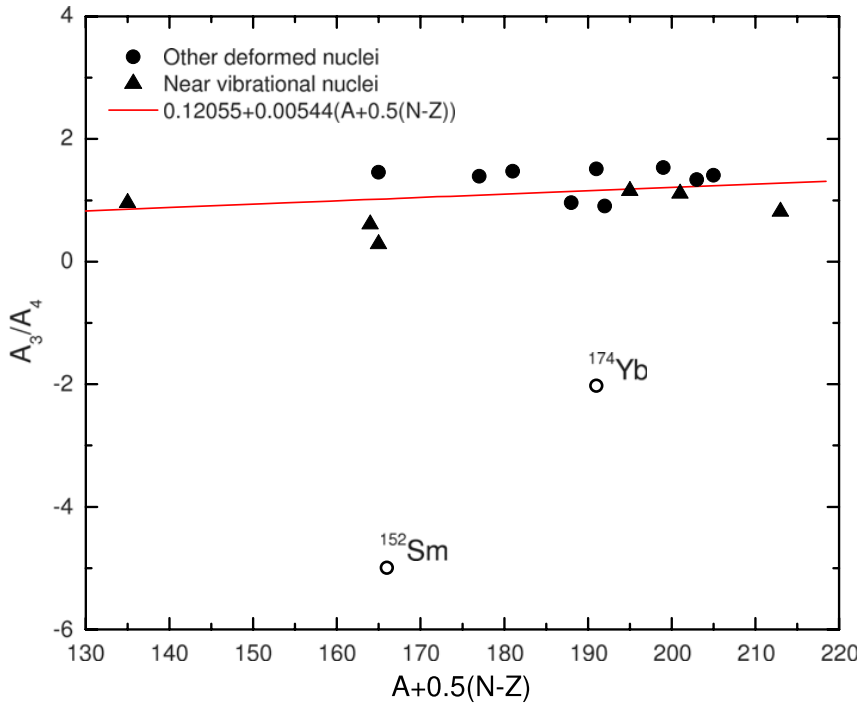

Fig. 9. For some nuclei, a good description of the excitation energies in the beta band is not possible unless the terms A_3 and A_4 are simultaneously considered. Here we plotted the ratio A_3/A_4 as function of $A + (N - Z)/2$. The resulting points were interpolated by a straight line.

parameter d is related linearly with the nuclear deformation β_2. The coefficients of the linear transformation are different for the three groups of nuclei: near vibrational, rare earth and transuranic nuclei.

5.2. $E2$ transition probabilities

For each considered nucleus, the two parameters defining the quadrupole transition operator were determined by a least squares fit of the experimental available data. As mentioned before, for the near vibrational limit the matrix elements of the transition operator $Q_{2\mu}$ were expanded as a power series of d from which we kept the terms non-depending on d and the next leading order terms which are in most cases linear in d. All matrix elements needed for describing the experimental situation were analytically expressed. The $B(E2)$ values are obtained by squaring the reduced matrix elements obtained as explained before. For near vibrational nuclei, the results are collected in Tables 5–8 where, for comparison, the corresponding experimental data are listed. We note that the limit $d \to 0$ provides similar results as the linear expansion in d for the transition operator. However, there are transitions which are forbidden in the vibrational limit but are described quantitatively well by the linear expansion of $Q_{2\mu}$. We remark that for the branching ratios given in Table 8, the results provided by the vibrational limit are in better agreement with the experimental data than those corresponding to a linear expansion of the transition operator. Moreover, some of the theoretical branching ratios are parameter independent. The agreement between the vibrational limit results and experimental data is especially good for ^{190}Pt which is considered to satisfy the $O(6)$ symmetry.

The $B(E2)$ values for the well deformed nuclei considered by the present work, have been calculated using the asymptotic expressions for the matrix elements given by Eqs. (4.21) and (4.22). The results are listed in Tables 9–12. As seen from these tables, a very good agreement between the results of our calculations and the corresponding experimental data is obtained. A special mention is deserved by ^{156}Gd, ^{158}Gd, ^{152}Sm and ^{232}Th where 25, 23, 22 and 20 $B(E2)$ values are available respectively, and an excellent agreement is obtained. Also for ^{172}Yb, ^{182}W and ^{186}Os, 17, 18 and 17 transitions respectively, are known and all of them are nicely described by the formalism proposed.

Author's personal copy

Table 5
$B(E2)$ transition probabilities for near vibrational nuclei ^{102}Pd [32], ^{154}Dy [35] and ^{152}Gd [34]. Values in square braces were not taken into account for the fitting procedure.

^{102}Pd				^{154}Dy				^{152}Gd			
$B(E2)$ [W.u.] $J_i^\pi \to J_f^\pi$	Exp.	Th. $d \to 0$	Th. Series of d	$B(E2)$[W.u.] $J_i^\pi \to J_f^\pi$	Exp.	Th. $d \to 0$	Th. Series of d	$B(E2)$[W.u.] $J_i^\pi \to J_f^\pi$	Exp.	Th. $d \to 0$	Th. Series of d
$2_g^+ \to 0_g^+$	32.6	18.27	20.69	$2_g^+ \to 0_g^+$	97	37.20	21.02	$2_g^+ \to 0_g^+$	73	60.88	76.00
$4_g^+ \to 2_g^+$	50.9	36.53	43.63	$4_g^+ \to 2_g^+$	157	74.40	164.89	$4_g^+ \to 2_g^+$	134	121.76	140.00
$2_\gamma^+ \to 2_g^+$	15	36.53	24.84	$6_g^+ \to 4_g^+$	199	111.60	194.50	$6_g^+ \to 4_g^+$	200	182.65	217.23
$2_\gamma^+ \to 0_g^+$	4.2	4.2	20.09	$8_g^+ \to 6_g^+$	220	148.80	197.30	$2_\beta^+ \to 0_\beta^+$	(42)	97.41	24.09
				$10_g^+ \to 8_g^+$	180	186.00	193.21	$0_\beta^+ \to 2_g^+$	180	180	58.61
				$12_g^+ \to 10_g^+$	170	223.20	191.74	$2_\beta^+ \to 0_g^+$	(0.31)	0	6.50
				$14_g^+ \to 12_g^+$	200	260.40	194.49	$2_\beta^+ \to 2_g^+$	(16.9)	0	61.05
								$2_\beta^+ \to 4_g^+$	[36]	81.00	41.16
d		0	1.45898	d		0	1.51491	d		0	1.53241
q_h $[(W.u.)^{\frac{1}{2}}]$		4.27391	5.78673	q_h $[(W.u.)^{\frac{1}{2}}]$		6.09923	94.8482	q_h $[(W.u.)^{\frac{1}{2}}]$		7.80268	2.19266
q_{anh} $[(W.u.)^{\frac{1}{2}}]$		1.44928	0.52039	q_{anh} $[(W.u.)^{\frac{1}{2}}]$		0	48.8486	q_{anh} $[(W.u.)^{\frac{1}{2}}]$		5.47727	6.41363

Table 6

$B(E2)$ transition probabilities for near vibrational nuclei ^{188}Os [36], ^{190}Os [37] and ^{192}Os [38]. Values in square braces were not taken into account for the fitting procedure.

^{188}Os				^{190}Os				^{192}Os			
$B(E2)$ [W.u.] $J_i^\pi \to J_f^\pi$	Exp.	Th. $d \to 0$	Th. Series of d	$B(E2)$[W.u.] $J_i^\pi \to J_f^\pi$	Exp.	Th. $d \to 0$	Th. Series of d	$B(E2)$[W.u.] $J_i^\pi \to J_f^\pi$	Exp.	Th. $d \to 0$	Th. Series of d
$2_g^+ \to 0_g^+$	79	28.72	27.10	$2_g^+ \to 0_g^+$	71.9	30.10	22.86	$2_g^+ \to 0_g^+$	64.4^{+7}_{-8}	23.80	23.85
$4_g^+ \to 2_g^+$	133	57.44	56.46	$4_g^+ \to 2_g^+$	105	60.20	46.67	$4_g^+ \to 2_g^+$	75.6	47.60	49.94
$6_g^+ \to 4_g^+$	(138)	86.15	85.79	$6_g^+ \to 4_g^+$	113	90.30	70.89	$6_g^+ \to 4_g^+$	100^{+5}_{-3}	71.40	75.72
$8_g^+ \to 6_g^+$	[161]	114.87	114.71	$8_g^+ \to 6_g^+$	137	120.40	94.97	$8_g^+ \to 6_g^+$	115	95.20	101.10
$10_g^+ \to 8_g^+$	[188]	143.59	143.57	$10_g^+ \to 8_g^+$	[120]	150.50	119.15	$10_g^+ \to 8_g^+$	105^{+9}_{-25}	119.00	126.41
$4_\gamma^+ \to 2_\gamma^+$	47	45.13	40.19	$4_\gamma^+ \to 2_\gamma^+$	53	47.30	19.25	$4_\gamma^+ \to 2_\gamma^+$	(45.3^{+14}_{-18})	37.40	41.19
$6_\gamma^+ \to 4_\gamma^+$	[70]	78.32	74.56	$6_\gamma^+ \to 4_\gamma^+$	[65]	82.09	40.05	$6_\gamma^+ \to 4_\gamma^+$	(52^{+3}_{-6})	64.91	74.41
$4_\gamma^+ \to 3_\gamma^+$	[320]	0	198.11	$8_\gamma^+ \to 6_\gamma^+$	[61]	114.38	60.73	$8_\gamma^+ \to 6_\gamma^+$	(48^{+7}_{-6})	90.44	105.58
$2_\gamma^+ \to 0_g^+$	5.0	0.79	10.88	$4_\gamma^+ \to 3_\gamma^+$	65	0	112.28	$2_\gamma^+ \to 0_g^+$	5.62^{+21}_{-12}	1.73	11.56
$2_\gamma^+ \to 2_g^+$	16	57.44	83.29	$2_\gamma^+ \to 0_g^+$	5.9	1.09	3.81	$2_\gamma^+ \to 2_g^+$	46.0^{+26}_{-12}	47.60	65.22
$2_\gamma^+ \to 4_g^+$	[34]	0	14.31	$2_\gamma^+ \to 2_g^+$	33	60.2	95.13	$4_\gamma^+ \to 2_g^+$	(0.2876^{+25}_{-34})	2.75	0.42
$4_\gamma^+ \to 2_g^+$	1.29	1.25	0.20	$4_\gamma^+ \to 2_g^+$	0.68	1.71	0.07	$4_\gamma^+ \to 4_g^+$	30.9^{+37}_{-18}	34.00	37.45
$4_\gamma^+ \to 4_g^+$	19	41.03	41.52	$4_\gamma^+ \to 4_g^+$	30	43.00	31.97	$6_\gamma^+ \to 6_g^+$	$[26.0^{+55}_{-21}]$	30.29	29.79
$4_\gamma^+ \to 6_g^+$	[16]	0	22.06	$6_g^+ \to 4_\gamma^+$	[6]	0	9.50	$0_\beta^+ \to 2_g^+$	[0.60]	5.25	0.61
$6_\gamma^+ \to 4_g^+$	[0.21]	1.70	0.01	$6_\gamma^+ \to 6_g^+$	[31]	38.31	19.10	$0_\beta^+ \to 2_\gamma^+$	$[30.4^{+30}_{-23}]$	71.40	66.92
$0_\beta^+ \to 2_g^+$	0.95	2.38	0.88	$0_\beta^+ \to 2_g^+$	2.2	3.26	1.33				
$0_\beta^+ \to 2_\gamma^+$	(4.3)	86.15	64.43	$0_\beta^+ \to 2_\gamma^+$	(23)	90.30	29.56				
d		0	1.62319	d		0	1.59990	d		0	1.61011
$q_h\,[(W.u.)^{\frac{1}{2}}]$		5.35888	5.02388	$q_h\,[(W.u.)^{\frac{1}{2}}]$		5.4863	3.85134	$q_h\,[(W.u.)^{\frac{1}{2}}]$		4.87841	4.96308
$q_{anh}\,[(W.u.)^{\frac{1}{2}}]$		0.62933	−0.35919	$q_{anh}\,[(W.u.)^{\frac{1}{2}}]$		0.737623	−0.71724	$q_{anh}\,[(W.u.)^{\frac{1}{2}}]$		0.93545	−0.20690

Author's personal copy

Author's personal copy

Table 7
$B(E2)$ transition probabilities for near vibrational nuclei ^{194}Pt [41], ^{196}Pt [42] and ^{186}Hg [40]. Values in square braces were not taken into account for the fitting procedure.

^{194}Pt				^{196}Pt				^{186}Hg			
$B(E2)$ [W.u.] $J_i^\pi \to J_f^\pi$	Exp.	Th. $d \to 0$	Th. Series of d	$B(E2)$[W.u.] $J_i^\pi \to J_f^\pi$	Exp.	Th. $d \to 0$	Th. Series of d	$B(E2)$[W.u.] $J_i^\pi \to J_f^\pi$	Exp.	Th. $d \to 0$	Th. Series of d
$2_g^+ \to 0_g^+$	49.3	27.22	25.56	$2_g^+ \to 0_g^+$	40.57	16.23	30.47	$2_g^+ \to 0_g^+$	44	55.44	57.05
$4_g^+ \to 2_g^+$	85	54.45	53.10	$4_g^+ \to 2_g^+$	59.9	32.47	61.57	$2_\beta^+ \to 0_\beta^+$	[400]	88.71	295.27
$6_g^+ \to 4_g^+$	67	81.67	79.20	$6_g^+ \to 4_g^+$	[73]	48.70	92.57	$4_\beta^+ \to 2_\beta^+$	[200]	152.47	286.29
$8_g^+ \to 6_g^+$	50	108.90	105.89	$8_g^+ \to 6_g^+$	[78]	64.93	124.39	$6_\beta^+ \to 4_\beta^+$	290	211.69	261.19
$4_\gamma^+ \to 2_\gamma^+$	22	42.78	52.31	$4_\gamma^+ \to 2_\gamma^+$	[29]	25.51	19.46	$8_\beta^+ \to 6_\beta^+$	$\approx$210	269.30	239.40
$2_\gamma^+ \to 0_g^+$	0.28	40.23	6.85	$6_\gamma^+ \to 4_\gamma^+$	49	44.27	41.44	$4_\beta^+ \to 2_g^+$	80	0	3.38
$2_\gamma^+ \to 2_g^+$	89	54.45	50.43	$2_\beta^+ \to 0_\beta^+$	[5]	25.97	39.80				
$4_\gamma^+ \to 2_g^+$	[0.22]	63.22	0.70	$2_\gamma^+ \to 0_g^+$	0.0158	0.65	0.04				
$4_\gamma^+ \to 4_g^+$	[20]	38.89	37.74	$4_\gamma^+ \to 2_g^+$	[0.56]	1.02	2.18				
$0_\beta^+ \to 2_g^+$	134	120.68	1.53	$6_\gamma^+ \to 4_g^+$	0.48	1.39	4.08				
$0_\beta^+ \to 2_\gamma^+$	135	81.67	89.62	$0_\beta^+ \to 2_g^+$	2.8	1.94	13.81				
				$2_\beta^+ \to 0_g^+$	[0.0025]	0	0.05				
				$2_\beta^+ \to 4_g^+$	[0.13]	2.43	6.39				
				$0_\beta^+ \to 2_\gamma^+$	18	48.70	29.80				
d		0	0.83137	d		0	0.95083	d		0	0.92388
$q_h\,[(W.u.)^{\frac{1}{2}}]$		5.21769	5.46832	$q_h\,[(W.u.)^{\frac{1}{2}}]$		4.02904	4.13681	$q_h\,[(W.u.)^{\frac{1}{2}}]$		7.44606	34.2497
$q_{anh}\,[(W.u.)^{\frac{1}{2}}]$		4.48486	0.09065	$q_{anh}\,[(W.u.)^{\frac{1}{2}}]$		0.56888	−1.43127	$q_{anh}\,[(W.u.)^{\frac{1}{2}}]$		0	35.7881

Table 8

Branching ratios for near vibrational nuclei ^{126}Xe [33], ^{182}Pt [39], ^{186}Pt [40] and ^{190}Pt [66].

^{126}Xe				^{182}Pt				^{186}Pt				^{190}Pt			
$\frac{B(E2;I\to I')}{B(E2;J\to J')}\times 10^{-2}$	Exp.	Th. $d\to 0$	Th. Series of d	$\frac{B(E2;I\to I')}{B(E2;J\to J')}$	Exp.	Th. $d\to 0$	Th. Series of d	$\frac{B(E2;I\to I')}{B(E2;J\to J')}\times 10^{-2}$	Exp.	Th. $d\to 0$	Th. Series of d	$\frac{B(E2;I\to I')}{B(E2;J\to J')}\times 10^{-2}$	Exp.	Th. $d\to 0$	Th Series of d
$\frac{2^+_\gamma\to 0^+_g}{2^+_\gamma\to 2^+_g}$	1.38	1.63	2.96	$\frac{2^+_\beta\to 2^+_g}{2^+_\beta\to 0^+_g}$	0.24	0	11.52	$\frac{2^+_\gamma\to 0^+_g}{2^+_\gamma\to 2^+_g}$	9.31	9.31	34.05	$\frac{2^+_\gamma\to 0^+_g}{2^+_\gamma\to 2^+_g}$	1.24	2.86	4.80
$\frac{0^+_\beta\to 2^+_g}{0^+_\beta\to 2^+_\gamma}$	9.27	3.25	9.25	$\frac{2^+_\gamma\to 2^+_g}{2^+_\gamma\to 0^+_g}$	<4.94	4.94	12.67	$\frac{2^+_\beta\to 0^+_g}{2^+_\beta\to 0^+_\beta}$	7.59	0	≈0	$\frac{3^+_\gamma\to 4^+_g}{3^+_\gamma\to 2^+_\gamma}$	49	40*	20.28
$\frac{3^+_\gamma\to 4^+_g}{3^+_\gamma\to 2^+_\gamma}$	85.60	40*	20.34					$\frac{2^+_\beta\to 0^+_g}{2^+_\beta\to 4^+_g}$	11.06	0	0.03	$\frac{3^+_\gamma\to 2^+_g}{3^+_\gamma\to 2^+_\gamma}$	1.8	5.73	11.83
$\frac{3^+_\gamma\to 2^+_g}{3^+_\gamma\to 2^+_\gamma}$	2.29	3.25	7.50					$\frac{4^+_\gamma\to 4^+_g}{4^+_\gamma\to 2^+_\gamma}$	42.03	90.91*	73.44	$\frac{0^+_\beta\to 2^+_g}{0^+_\beta\to 2^+_\gamma}$	11	16.20	2.63
$\frac{4^+_\gamma\to 4^+_g}{4^+_\gamma\to 2^+_\gamma}$	86.33	90.91*	93.98					$\frac{4^+_\beta\to 2^+_g}{4^+_\beta\to 2^+_\beta}$	2.61	0	≈0	$\frac{2^+_\beta\to 0^+_g}{2^+_\beta\to 0^+_\beta}$	0.2	0	≈0
$\frac{4^+_\gamma\to 2^+_g}{4^+_\gamma\to 2^+_\gamma}$	1.09	3.25	0.18									$\frac{2^+_\beta\to 4^+_g}{2^+_\beta\to 0^+_\beta}$	4.2	4.83	4.13
$\frac{5^+_\gamma\to 4^+_\gamma}{5^+_\gamma\to 3^+_\gamma}$	94.04	45.45*	46.20												
$\frac{5^+_\gamma\to 4^+_g}{5^+_\gamma\to 3^+_\gamma}$	3.76	4.64	1.79												
$\frac{6^+_\gamma\to 6^+_g}{6^+_\gamma\to 4^+_\gamma}$	86.19	46.67*	41.16												
$\frac{6^+_\gamma\to 4^+_g}{6^+_\gamma\to 4^+_\gamma}$	0.63	2.55	0.45												
d		0	0.67610	d		0	1.69634	d		0	1.67744	d		0	0.74815
q_{anh}/q_h		0.12749	−0.10137	q_{anh}/q_h		0.450	0.60093	q_{anh}/q_h		0.30512	0.00418	q_{anh}/q_h		0.16922	−0.07169

* Do not depend on any parameters.

Author's personal copy

Author's personal copy

Table 9
$B(E2)$ transition probabilities in the asymptotic limit for deformed Gd nuclei. Values in square braces were not taken into account for the fitting procedure. Experimental data are taken from [34,35,44–47].

$B(E2)$ tr. prob.	^{154}Gd		^{156}Gd		^{158}Gd		^{160}Gd	
$J_i^\pi \to J_f^\pi$	Exp.	Th.	Exp.	Th.	Exp.	Th.	Exp.	Th.
$2_g^+ \to 0_g^+$	157	161.4021	187	181.9295	198	200.4643	201.2	200.5707
$4_g^+ \to 2_g^+$	245	230.5744	263	259.8993	289	286.3776		
$6_g^+ \to 4_g^+$	285	253.9543	295	286.2527				
$8_g^+ \to 6_g^+$	[312]	265.8387	320	299.6486	[330]	330.1765		
$10_g^+ \to 8_g^+$			314	307.7755	340	339.1314		
$12_g^+ \to 10_g^+$			300	313.2351	[310]	345.1473		
$2_\beta^+ \to 0_\beta^+$	97	161.4021	[52]	181.9295				
$4_\beta^+ \to 2_\beta^+$			280	259.8993	[455]	286.3776		
$4_\gamma^+ \to 2_\gamma^+$					[113]	119.3240		
$5_\gamma^+ \to 3_\gamma^+$			100^{+3}_{-1}	173.6600				
$0_\beta^+ \to 2_g^+$	52	46.2919	8	7.4675	1.1652	2.2242		
$2_\beta^+ \to 0_g^+$	0.86	9.2584	0.63	1.4935	0.31	0.4448		
$2_\beta^+ \to 2_g^+$	6.7	13.2263	3.3	2.1336	0.079	0.6355		
$2_\beta^+ \to 4_g^+$	19.6	23.8073	4.1	3.8404	1.39	1.1439		
$4_\beta^+ \to 2_g^+$			1.3	2.1336	1.32	0.6355		
$4_\beta^+ \to 4_g^+$					0.37	0.5777		
$4_\beta^+ \to 6_g^+$			2.1	3.3943	3.16	1.0110		
$2_\gamma^+ \to 0_g^+$	5.7	10.8613	4.68	9.5440	3.4	9.1615	3.80	9.1323
$2_\gamma^+ \to 2_g^+$	12.3	15.5162	7.24	13.6343	6.0	13.0879	7.1	13.0461
$2_\gamma^+ \to 4_g^+$	1.72	0.7758	0.77	0.6817	(0.27)	0.6544	0.72	0.6523
$3_\gamma^+ \to 2_g^+$			7.3	17.0428	3.5	16.3599		
$3_\gamma^+ \to 4_g^+$			5.1	6.8171	1.77	6.5439		
$4_\gamma^+ \to 2_g^+$			1.8	5.6809	1.13	5.4533		
$4_\gamma^+ \to 4_g^+$			10	16.7329	7.31	16.0624		
$4_\gamma^+ \to 6_g^+$					[0.949]	1.3881		
$5_\gamma^+ \to 4_g^+$			8^{+16}_{-8}	15.1836				
$5_\gamma^+ \to 6_g^+$			11^{+23}_{-11}	8.6763				
$2_\gamma^+ \to 0_\beta^+$	[1.21]	0.1270						
$4_\gamma^+ \to 2_\beta^+$			[4.3]	0.0664				
$4_\beta^+ \to 2_\gamma^+$					[12.8]	0.0043		
d	2.72583		3.08725		3.30765		3.31382	
$q_h\,[(W.u.)^{\frac{1}{2}}]$	5.21088		4.88466		4.78579		4.77815	
$q_{anh}\,[(W.u.)^{\frac{1}{2}}]$	5.60468		2.25107		1.22853		0	

It is worth mentioning that the list of nuclei considered in the present paper include isotopes of various "nuclear phases" with specific symmetries like gamma stable, gamma unstable, triaxial shape, deformed axial symmetric nuclei showing a $SU(3)$ symmetry, critical nuclei of various phase transitions satisfying the symmetries $E(5)$ (^{102}Pd) and $X(5)$ (^{152}Sm, ^{154}Gd) respectively. In the isotopic chain of $^{152-162}$Gd, two phase transitions take place namely from $SU(5)$ to $SU(3)$ with the critical nucleus ^{154}Gd and from $SU(3)$ to O (6), i.e. to a gamma unstable shape, the critical nucleus being ^{160}Gd [28]. The properties of all these nuclei can be described fairly well by CSM. Moreover, in this work, we present analytical expressions for energies and transition probabilities for vibrational, transitional and well deformed nuclei. Since the analytical formulas are easy to be handled, and by this paper they were positively tested, we may say that the results presented here represent a major achievement of CSM.

6. Conclusions

The present paper considers the CSM approach in two extremes of small and large deformations. Thus, the matrix elements of the model Hamiltonian as well as of the $E2$ transition operator between

Author's personal copy

Table 10
$B(E2)$ transition probabilities in the asymptotic limit for few deformed transuranic nuclei which have absolute experimental values also for inter-band transitions. Values in square braces were not taken into account for the fitting procedure. Only for ^{230}Th and ^{238}Pu were used the uncertain β-ground transition probabilities in order to fix the q_{anh} parameter. Experimental data are taken from [50,51,54].

$B(E2)$ tr. prob.	^{230}Th		^{232}Th		^{238}U		^{238}Pu	
$J_i^\pi \to J_f^\pi$	Exp.	Th.	Exp.	Th.	Exp.	Th.	Exp.	Th.
$2_g^+ \to 0_g^+$	192	185.3438	198	223.2176	281	280.2843	285	285
$4_g^+ \to 2_g^+$	261	264.7768	286	318.8822				
$6_g^+ \to 4_g^+$			327	351.2164				
$8_g^+ \to 6_g^+$			343	367.6524	$[404^{+67}_{-47}]$	400.4061		
$10_g^+ \to 8_g^+$			361	377.6237	$[480^{+61}_{-48}]$	474.1651		
$12_g^+ \to 10_g^+$			370	384.3224	[500]	482.5765		
$14_g^+ \to 12_g^+$			390	389.1341	[491]	488.6182		
$16_g^+ \to 14_g^+$			390	392.7582				
$18_g^+ \to 16_g^+$			440	395.5863	[480]	496.7200		
$20_g^+ \to 18_g^+$			360	397.8550	[460]	499.5687		
$22_g^+ \to 20_g^+$			420	399.7152	[490]	501.9044		
$24_g^+ \to 22_g^+$			240	401.2682				
$26_g^+ \to 24_g^+$			350	402.5844				
$28_g^+ \to 26_g^+$			705	403.7141				
$2_\beta^+ \to 0_g^+$	[1.1]	1.1223	2.3	1.0374	[0.38]	0.7	[3.9]	1.5595
$2_\beta^+ \to 2_g^+$			$\approx$0.	1.4820	1.0	1.0		
$2_\beta^+ \to 4_g^+$	[3.8]	2.8859	[$\approx$3.]	2.6676	[3.3]	1.8	[3.1]	4.0102
$2_\gamma^+ \to 0_g^+$	3.0	8.9506	3.0	9.8088	3.04	10.0168		
$2_\gamma^+ \to 2_g^+$	5.4	12.7866	7.1	14.0126	5.3	14.3097		
$2_\gamma^+ \to 4_g^+$	[0.35]	0.6393	$\approx$0.	0.7006	0.33	0.7155		
d	3.21904		3.37319		3.74042		3.96825	
$q_h\ [(W.u.)^{\frac{1}{2}}]$	4.73039		4.95197		5.00419		4.75640	
$q_{anh}\ [(W.u.)^{\frac{1}{2}}]$	1.95136		2.25107		1.54111		2.30027	

the angular momentum projected states modeling the members of the ground, beta and gamma bands, are alternatively expanded in power series of $x(=d^2)$ and $1/x$. As a result the excitation energies in the three bands are expressed analytically as ratios of polynomials in x and $1/x$ respectively with the coefficients depending on angular momentum. Concerning the matrix elements of the $E2$ transition operator, for small deformation they are, with a few exceptions, linear functions in d, the expansion coefficients being rational functions of the angular momentum. In the large deformation regime, the whole angular momentum dependence of the mentioned matrix elements is contained by a Clebsch–Gordan coefficient which is accompanied by a factor depending on d for intraband and independent of deformation for interband transitions.

This simple description is used to describe the available data for 42 nuclei exhibiting various symmetries like $SU(5)$, $O(6)$, $SU(3)$, triaxial shapes. The results are in a good agreement with the corresponding experimental data for both excitation energies for the three bands and the transition probabilities. Note that for all symmetries mentioned above we use a sole Hamiltonian and a sole set of projected states. The distinct features of each symmetry are obtained by a specific deformation parameter and structure coefficients. Changing the nucleus under consideration, the coefficients are not changing chaotically but obey a certain rule expressed by their dependence on $A + (N - Z)/2$. In fact this is a measure of the predictability power of the CSM approach. As shown for the Gd isotopes, CSM describes not only the nuclei corresponding to a certain symmetry but also those corresponding to the transition between them including the critical nucleus.

Comparing CSM with the Liquid Drop Model (LDM), one may say that CSM is a highly anharmonic model while LDM has a harmonic structure. However, as we mentioned before in the large deformation situation, the CSM wave functions are similar to those characterizing

Author's personal copy

Table 11
$B(E2)$ transition probabilities in the asymptotic limit for lightest rare earth nuclei. Values in square braces were not taken into account for the fitting procedure. The uncertain transition probabilities were used for ^{150}Nd in order to make the fit. Experimental data are taken from [58,34,59–61].

$B(E2)$ tr. prob.	^{150}Nd		^{152}Sm		^{162}Dy		^{164}Dy		^{166}Er	
$J_i^\pi \to J_f^\pi$	Exp.	Th.	Exp.	Th.	Exp.	Th.	Exp.	Th.	Exp.	Th.
$2_g^+ \to 0_g^+$	[115]	131.9577	144	183.2375	199	192.5001	209	198.8182	214	219.0829
$4_g^+ \to 2_g^+$	[175]	188.5110	209	261.7679	288	275.0002	272	284.0207	311	312.9756
$6_g^+ \to 4_g^+$	[212]	207.6258	245	288.3108	300	302.8848	325	312.8259	347	344.9756
$8_g^+ \to 6_g^+$	[236]	217.3421	285	301.8030	[347]	317.0590	310	327.4653	365	360.8425
$10_g^+ \to 8_g^+$			320	309.9883	[350]	325.6581	354	336.3466	371	370.6290
$12_g^+ \to 10_g^+$					320	331.4350	356	342.3132	376	377.2037
$14_g^+ \to 12_g^+$					330	335.5845	326	346.5988		
$2_\beta^+ \to 0_\beta^+$			[520]	183.2375						
$4_\beta^+ \to 2_\beta^+$			≈400	261.7679						
$4_\gamma^+ \to 2_\gamma^+$			[50]	109.0700						
$0_\beta^+ \to 2_g^+$	[0.0428]	8.9884	32.7	28.2136						
$2_\beta^+ \to 0_g^+$	[0.51]	1.7977	0.92	5.6427						
$2_\beta^+ \to 2_g^+$	[7.1]	2.5681	5.5	8.0610						
$2_\beta^+ \to 4_g^+$	[20]	4.6226	(19.0)	14.5098						
$4_\beta^+ \to 2_g^+$			≈1.0	8.0610						
$4_\beta^+ \to 4_g^+$			≈9.0	7.3282						
$4_\beta^+ \to 6_g^+$			(≈6.0)	12.8243						
$2_\gamma^+ \to 0_g^+$	[3.0]	9.7248	3.62	12.8838	[0.0241]	8.9188	4.0	10.6601	5.5	12.6207
$2_\gamma^+ \to 2_g^+$	[5.7]	13.8926	9.3	18.4054	≈0	12.7411	8.0	15.2288	9.7	18.0296
$2_\gamma^+ \to 4_g^+$	[1.7]	0.6946	(0.78)	0.9203	[0.00330]	0.6371	0.96	0.7614	0.67	0.9015
$4_\gamma^+ \to 2_g^+$			0.59	7.6689						
$4_\gamma^+ \to 4_g^+$			5.5	22.5885						
$4_\gamma^+ \to 6_g^+$			[1.2]	1.9521						
$4_\gamma^+ \to 2_\beta^+$			[0.18]	0.0897						
d	2.60473		2.66667		3.28509		3.05374		2.94610	
$q_h\,[(W.u.)^{\frac{1}{2}}]$	4.93072		5.67534		4.72197		5.16240		5.61710	
$q_{anh}\,[(W.u.)^{\frac{1}{2}}]$	2.46967		4.37549		0		0		0	

LDM in the strong coupling limit. Another successful anharmonic model was proposed by Gneus and Greiner but that uses a large number of parameters and moreover, the quadrupole conjugate momenta contribute to the Hamiltonian only through the quadratic terms. Moreover, energies are obtained by the diagonalization procedure in a spherical basis which may encounter convergence difficulties for large deformations. By contrast, CSM projects, over angular momentum, states from a coherent state and two orthogonal polynomial excitations and consequently is especially realistic for the well deformed nuclei. This feature is actually confirmed by the application from this paper where the transuranic nuclei spectra are obtained with a high accuracy.

CSM accounts for features which are complementary to those described by IBA. Indeed CSM's model Hamiltonian is not a boson number conserving Hamiltonian. Moreover, while IBA uses a space of states with limited number of bosons, CSM states cover the whole boson space since they are projected from infinite series of bosons. Due to this feature, the IBA approach is concerned with the description of low lying states with angular momentum not exceeding 12^+ and with a moderate deformation. By contrast, CSM works quite well for high spin states (in Fig. 3 energies for states with $J \leq 32$ are shown). CSM was applied for the description of the triaxial nuclei [67] and the results were compared with those obtained within the Vibration Rotation Model [2]. Recently, a more extensive study of triaxial nuclei with CSM has been performed [68] and the results were compared with those produced by a solvable model.

The results of the present paper are quite encouraging for continuing the study of CSM to unveil new virtues suitable to describe even more complex experimental data.

Table 12
$B(E2)$ transition probabilities in the asymptotic limit for heaviest rare earth nuclei. Values in square braces were not taken into account for the fitting procedure. Experimental data are taken from [39,40,62–65].

$B(E2)$ tr. prob.	^{172}Yb		^{174}Yb		^{176}Hf		^{182}W		^{186}W		^{186}Os	
$J_i^\pi \to J_f^\pi$	Exp.	Th.	Exp.	Th.	Exp.	Th.	Exp.	Th.	Exp.	Th.	Exp.	Th.
$2_g^+ \to 0_g^+$	212	226.1302	201	214.4049	183	182.7660	137	119.5874	111	100.9240	92.3	94.6028
$4_g^+ \to 2_g^+$	301	323.0431	280	306.2927			196	170.8392	144	144.1772	134	135.1469
$6_g^+ \to 4_g^+$	320	355.7992	370	337.3503			200	188.1620	187	158.7966	184	148.8506
$8_g^+ \to 6_g^+$	400	372.4497	[388]	353.1374			209	196.9675	178	166.2278	174	155.8164
$10_g^+ \to 8_g^+$	375	382.5510	[335]	362.7150			203	202.3095	151^{+15}_{-45}	170.7362	190	160.0424
$12_g^+ \to 10_g^+$	(400)	389.3372	[369]	369.1493			191	205.8983	189^{+20}_{-56}	173.7649	170	162.8814
$14_g^+ \to 12_g^+$	$\left(394^{+60}_{-45}\right)$	394.2116	[320]	373.7709			(170)	208.4761	138	175.9404		
$16_g^+ \to 14_g^+$							[204]	210.4177				
$18_g^+ \to 16_g^+$							[250]	211.9329				
$2_\beta^+ \to 0_\beta^+$							[200]	119.5874				
$4_\gamma^+ \to 2_\gamma^+$											72	56.3112
$6_\gamma^+ \to 4_\gamma^+$											119	111.1418
$8_\gamma^+ \to 6_\gamma^+$											79	134.1532
$10_\gamma^+ \to 8_\gamma^+$											89	146.0535
$0_\beta^+ \to 2_g^+$	[3.6]	4.0387	$[1.4^{+11}_{-5}]$	1.4								
$2_\beta^+ \to 0_g^+$	0.24	0.8077			1.0	2.0568	0.91	0.6483				
$2_\beta^+ \to 2_g^+$	0.79	1.1539					0.63	0.9262				
$2_\beta^+ \to 4_g^+$	2.5	2.0770			5.7	5.2890	1.73	1.6672				
$2_\gamma^+ \to 0_g^+$	1.33	8.2744			4.1	8.9042	3.40	5.8162	4.63	7.5447	10.1	8.3604
$2_\gamma^+ \to 2_g^+$			2.5	10.6707			6.74	8.3089	10.1	10.7781	23.5	11.9435
$2_\gamma^+ \to 4_g^+$	(0.129)	0.5910					0.0339	0.4154			[1.2]	0.5972
$4_\gamma^+ \to 2_g^+$	7	4.9252					2.35	3.4620			3.2	4.9764
$4_\gamma^+ \to 4_g^+$	13	14.5070					10.4	10.1973			24.7	14.6579
$6_\gamma^+ \to 4_g^+$											1.27	4.0925
$6_\gamma^+ \to 6_g^+$											18.5	15.2008
$2_\gamma^+ \to 0_\beta^+$	[2.42]	1.3344										
$2_\gamma^+ \to 2_\beta^+$	[3.4]	1.9064										
d	3.69655		3.78841		3.20357		3.20632		2.58620		2.37861	
q_h $[(W.u.)^{\frac{1}{2}}]$	4.54818		4.32131		4.71811		3.81321		4.34301		4.57177	
q_{anh} $[(W.u.)^{\frac{1}{2}}]$	1.65546		0.97468		2.64170		1.48316		0		0	

Author's personal copy

Author's personal copy

Acknowledgment

This work was supported by the Romanian Ministry for Education, Research, Youth and Sport through the CNCSIS project ID-1038/2008.

Appendix A

Coefficients of the near vibrational energy formulas are given as follows:

$$\sum_{k=0}^{3} Q_{J,k}^{(\gamma,0)} x^k = \frac{(J+1)(J+2)(2J+3)}{6(J-1)} + \frac{(J+2)(7J^2+7J-24)}{(J-1)(2J+3)}x + \frac{3}{2}\frac{20J^4+85J^3+85J^2+38J+42}{(J-1)(2J+3)^2(2J+5)}x^2 + \frac{9(J+1)(14J^4+84J^3+108J^2-122J-204)}{(J-1)(2J+3)^3(2J+5)(2J+7)}x^3, \tag{A.1}$$

$$\sum_{k=0}^{3} Q_{J,k}^{(\gamma,1)} x^k = (J+2)^2 + \frac{9J^3+22J^2-10J-6}{(2J+1)(2J+3)}x + \frac{3J(12J^3+53J^2+81J+22)}{(2J+1)^2(2J+3)(2J+5)}x^2 + \frac{9J(3J+5)}{(2J+1)^2(2J+3)(2J+5)}x^3, \tag{A.2}$$

$$\sum_{k=0}^{3} R_{J,k}^{(\gamma,0)} x^k = \frac{1}{12(J-1)}(J-2)(J+1)(J+2)(2J+3) + \frac{44J^5+199J^4+67J^3-748J^2-948J-144}{12(J-1)(J+2)(2J+3)}x + \left[\frac{1}{J+2}(22J^4+59J^3-J^2+82J+288) + \frac{3(J+1)}{(2J+3)(2J+5)}(2J^4+4J^3-5J^2-7J-24)\right] \times \frac{x^2}{4(J-1)(2J+3)} + \left[\frac{9(J+1)(34J^4+196J^3+99J^2-959J-1200)}{(2J+3)^2(2J+5)(2J+7)} + \frac{39J^3+81J^2-54J-120}{J+2}\right]\frac{x^3}{4(J-1)(2J+3)}, \tag{A.3}$$

$$\sum_{k=0}^{3} R_{J,k}^{(\gamma,1)} x^k = \frac{1}{2}(J-1)(J+2)^2 + \frac{11J^4+24J^3-43J^2-100J-42}{2(2J+1)(2J+3)}x + \frac{9J^3+25J^2+38J+3}{(2J+1)(2J+3)}x^2 + \frac{9}{2}\frac{J(J-1)^2(J+2)}{(2J+1)^2(2J+3)(2J+5)}x^2 + 3\frac{J(12J^3+41J^2+36J+31)}{(2J+1)^2(2J+3)(2J+5)}x^3, \tag{A.4}$$

$$\sum_{k=1}^{3} U_{J,k}^{(\gamma,0)} x^k = \frac{4J(J+1)(J+2)}{15(J-1)}x - \frac{8(J+1)(J+2)(J-3)}{5(J-1)(2J+3)}x^2 + \frac{12}{5}\frac{4J^4+23J^3+5J^2-110J-120}{(J-1)(2J+3)^2(2J+5)}x^3, \tag{A.5}$$

$$\sum_{k=2}^{3} U_{J,k}^{(\gamma,1)} x^k = \frac{16}{5}x^2 - \frac{48}{5}\frac{J}{(J+1)(2J+3)}x^3, \tag{A.6}$$

Author's personal copy

$$\sum_{k=0}^{3} Q_{J,k}^{(\beta)} x^k = 3J + 10 + \frac{3}{7}\frac{17J+15}{2J+3}x + 27\frac{(J+1)(J+2)}{(2J+3)^2(2J+5)}x^2 + 81\frac{(J+1)(J+2)}{(2J+3)^3(2J+5)(2J+7)}x^3, \tag{A.7}$$

$$\sum_{k=0}^{3} R_{J,k}^{(\beta)} x^k = \frac{3}{2}J^2 + 14J + 30 + \frac{72J^2+403J+180}{14(2J+3)}x + \frac{3}{14}\frac{160J^3+1333J^2+2847J+1680}{(2J+3)^2(2J+5)}x^2 + \frac{27}{14}\frac{(J+1)(J+2)(48J^2+240J+427)}{(2J+3)^3(2J+5)(2J+7)}x^3, \tag{A.8}$$

$$\frac{35}{6}\sum_{k=0}^{3} U_{J,k}^{(\beta)} x^k = 2J(2J+3) + \frac{-12J^2+34J+75}{2J+3}x + \frac{2(52J^3+313J^2+606J+378)}{(2J+3)^2(2J+5)}x^2 - 216\frac{(J+1)(J+2)(J^2+5J+5)}{(2J+3)^3(2J+5)(2J+7)}x^3, \tag{A.9}$$

$$\sum_{k=0}^{3} V_{J,k}^{(\beta)} x^k = \frac{3}{5}(9J^2+60J+100) + \frac{18}{35}\frac{51J^2+236J+150}{2J+3}x + \frac{27}{245}\left[123 + 119\frac{4J^3+37J^2+78J+42}{(2J+3)^2(2J+5)}\right]x^2 + \frac{16524}{35}\frac{(J+1)(J+2)(J^2+5J+7)}{(2J+3)^3(2J+5)(2J+7)}x^3, \tag{A.10}$$

$$\sum_{k=1}^{3} B_{J,k}^{(\beta)} x^k = \frac{96}{175}\left[J^2 x - \frac{2J(J+2)}{2J+3}x^2 + \frac{20J^3+107J^2+192J+117}{(2J+3)^2(2J+5)}x^3\right], \tag{A.11}$$

$$\sum_{k=0}^{3} Z_{J,k}^{(\beta)} x^k = \frac{48}{5\sqrt{70}}\left[-(3J^2+46J+120) + \left(Q_{J,0}^{(\beta)} - \frac{72J^2+649J+360}{7(2J+3)}\right)x + \left(Q_{J,1}^{(\beta)} - \frac{3}{7}\frac{160J^3+1711J^2+3981J+2436}{(2J+3)^2(2J+5)}\right)x^2 + \left(Q_{J,2}^{(\beta)} - \frac{27}{7}\frac{(J+1)(J+2)(48J^2+240J+553)}{(2J+3)^3(2J+5)(2J+7)}\right)x^3\right], \tag{A.12}$$

$$\sum_{k=1}^{3} T_{J,k} x^k = 242\frac{J(J+1)(J+2)}{J-1}\left[\frac{x}{6} - \frac{x^2}{2J+3} + \frac{3}{2}\frac{4J+7}{(2J+3)^2(2J+5)}x^3\right], \tag{A.13}$$

$$\sum_{k=0}^{3} X_{J,k} x^k = \frac{(J+1)(J+2)(2J+3)}{6(J-1)} + \frac{3(4J^3+11J^2-11J-34)}{(J-1)(2J+3)}x + \left[-\frac{88J^5+196J^4-460J^3-973J^2-585J-396}{4(J-1)(2J+3)^2(2J+5)} + \frac{22J^3+15J^2-31J+144}{4(J-1)(2J+3)}\right]x^2 + \frac{9}{4}\left[\frac{(J+1)(-28J^5-24J^4+639J^3+1176J^2-1559J-2844)}{(J-1)(2J+3)^3(2J+5)(2J+7)} + \frac{14J^5+81J^4+137J^3-13J^2-191J-108}{(J-1)(2J+3)^3(2J+5)}\right]x^3. \tag{A.14}$$

Author's personal copy

The term ΔE_J accounts for the interaction between the states ϕ^g_{JM} and ϕ^γ_{JM}. In the near vibrational regime this has the expression

$$\Delta E_J = A_1 \frac{\sum_{k=0}^{3} T_{J,k} x^k}{\sum_{k=0}^{3} \left(22X_{J,k} + 5U^{(\gamma,0)}_{J,k}\right) x^k}, \tag{A.15}$$

with coefficients $T_{J,k}$ and $X_{J,k}$ given above.

Appendix B

$$P^\beta_J = \frac{12}{5} + \frac{171}{35}x - \frac{6}{5x} + \left(\frac{3}{5x} + \frac{1}{x^2} + \frac{13}{5x^3}\right)J(J+1) - \frac{1}{15x^3}J^2(J+1)^2, \tag{B.1}$$

$$\begin{aligned} S^\beta_J &= \frac{2}{35}\left[1917x^2 + 5946x + 759 - \frac{1937}{x}\right] \\ &\quad + \frac{J(J+1)}{35}\left[1125 + \frac{2537}{x} + \frac{14365}{3x^2} + \frac{25181}{3x^3}\right] - \frac{J^2(J+1)^2}{7x^2}\left(8 + \frac{1937}{45x}\right), \end{aligned} \tag{B.2}$$

$$\begin{aligned} F^\beta_J &= \frac{54}{1225}\left[-\frac{406}{3} + \frac{1083}{2}x^2 + 826x - \frac{833}{3x} + \left(133 + \frac{714}{3x} + \frac{4403}{9x^2}\right.\right. \\ &\quad \left.\left. + \frac{10829}{18x^3}\right)J(J+1) - \frac{119}{18x^2}\left(1 + \frac{7}{3x}\right)J^2(J+1)^2\right]. \end{aligned} \tag{B.3}$$

For J = odd, we have

$$\begin{aligned} S^\gamma_J &= 198(J+1)x^3 + (J+1)(-66J + 368)x^2 + (J+1)\left(77J^2 - \frac{335}{3}J - \frac{188}{3}\right)x \\ &\quad + \frac{1}{9}(-165J^4 + 1023J^3 + 635J^2 - 2219J - 2046) \\ &\quad + \frac{(J-1)}{27x}(33J^4 - 688J^3 + 4549J^2 + 7098J - 396) \\ &\quad + \frac{11J(J-1)}{27x^2}(2J^4 + 3J^3 - 162J^2 + 499J + 1296) \\ &\quad - \frac{11}{27x^3}J(J-1)^3(J-2)(J^2 - J - 39), \end{aligned} \tag{B.4}$$

$$\begin{aligned} P^\gamma_J &= 9(J+1)x^2 - (3J-4)(J+1)x + \frac{1}{3}(J+1)(6J^2 - 7J - 7) \\ &\quad + \frac{1}{9x}(J-1)(-3J^3 + 21J^2 + 28J - 6) \\ &\quad + \frac{1}{x^2}J(J-1)\left(-\frac{1}{9}J^3 - \frac{17}{27}J^2 + \frac{152}{27}J + \frac{20}{3}\right) + \frac{J(J-1)^3}{27x^3}(J^2 - J - 39). \end{aligned} \tag{B.5}$$

For J = even, we have

$$S^\gamma_J = \sum_{k=0}^{4} U^{(k)} J^k (J+1)^k, \qquad P^\gamma_J = \sum_{k=0}^{3} V^{(k)} J^k (J+1)^k, \tag{B.6}$$

Author's personal copy

where

$$
\begin{aligned}
U^{(0)} &= -396x^3 - 736x^2 + \frac{376}{3}x + \frac{1364}{3} - \frac{88}{3x},\\
U^{(1)} &= 198x^3 + 368x^2 - \frac{584}{3}x - \frac{3835}{9} - \frac{4655}{9x} - \frac{1056}{x^2} + \frac{572}{9x^3},\\
U^{(2)} &= 66x + \frac{1037}{9} + \frac{5702}{27x} + \frac{18847}{54x^2} + \frac{451}{6x^3},\\
U^{(3)} &= -\frac{47}{54x} - \frac{49}{9x^2} + \frac{539}{162x^3},\\
U^{(4)} &= -\frac{11}{81x^3},
\end{aligned}
\tag{B.7}
$$

$$
\begin{aligned}
V^{(0)} &= -18x^2 - 8x + \frac{14}{3} - \frac{4}{3x},\\
V^{(1)} &= 9x^2 + 4x - \frac{16}{3} - \frac{53}{9x} - \frac{40}{3x^2} + \frac{26}{9x^3},\\
V^{(2)} &= \frac{3}{2} + \frac{22}{9x} + \frac{169}{27x^2} + \frac{113}{54x^3},\\
V^{(3)} &= -\frac{7}{54x^2} - \frac{1}{18x^3}.
\end{aligned}
\tag{B.8}
$$

The factors $T_J^{n,\beta}$, with $n = 4, 5$, involved in the equation determining the excitation energies in the beta band have the following expression:

$$
\begin{aligned}
T_J^{4,\beta} &= \frac{171}{35}x^2 + \frac{195}{7}x + \frac{321}{35} - \frac{361}{35x} - \frac{1949}{105x^2} - \frac{1591}{45x^3}\\
&\quad + J(J+1)\left(\frac{99}{70} + \frac{361}{70x} + \frac{1973}{210x^2} + \frac{559}{30x^3}\right) - \frac{1}{54x^3}\left(\frac{129}{5} + \frac{108}{35}x\right)J^2(J+1)^2,\\
T_J^{5,\beta} &= \left[9x^3 + 24x + 16 + \frac{104}{3x} + \frac{74}{3x^2} + \left(6x - 8 - \frac{18}{x} - \frac{13}{x^2}\right)J(J+1)\right.\\
&\quad \left. + \frac{x+1}{3x^2}J^2(J+1)^2\right].
\end{aligned}
\tag{B.9}
$$

Appendix C

The exact m.e. of the harmonic part of the quadrupole transition operator [5] can be expressed in terms of the projected state norms:

$$
\langle \phi_J^g || Q_2^h || \phi_{J'}^g \rangle = q_h d C_{000}^{J'2J}\left[\frac{2J'+1}{2J+1}\frac{N_{J'}^g}{N_J^g} + \frac{N_J^g}{N_{J'}^g}\right],
\tag{C.1}
$$

$$
\langle \phi_J^\beta || Q_2^h || \phi_{J'}^\beta \rangle = q_h d C_{000}^{J'2J}\left[\frac{N_J^\beta}{N_{J'}^\beta} + \frac{18}{5}\frac{N_J^\beta N_{J'}^\beta}{(N_{J'}^g)^2} + \frac{2J'+1}{2J+1}\left(\frac{N_{J'}^\beta}{N_J^\beta} + \frac{18}{5}\frac{N_J^\beta N_{J'}^\beta}{(N_J^g)^2}\right)\right],
\tag{C.2}
$$

$$
\langle \phi_J^g || Q_2^h || \phi_{J'}^\beta \rangle = 0,
\tag{C.3}
$$

Author's personal copy

$$\langle\phi_J^\gamma||Q_2^h||\phi_{J'}^g\rangle = q_h d N_J^\gamma \left[\sqrt{\frac{2}{7}}C_{022}^{J'2J}\frac{1}{N_{J'}^g} + 2\sum_{J_1}\hat{2}\hat{J}C_{-220}^{2JJ_1}C_{000}^{J'2J_1} \times W(22JJ';2J_1)\frac{2J'+1}{2J_1+1}\frac{N_{J'}^g}{\left(N_{J_1}^g\right)^2}\right], \tag{C.4}$$

$$\langle\phi_J^\beta||Q_2^h||\phi_{J'}^\gamma\rangle = q_h N_J^\beta N_{J'}^\gamma (2J'+1)\frac{6}{7\sqrt{5}}\left\{C_{2-20}^{J'2J}\frac{1}{2J+1} \times\left[3\left(\frac{2}{7}d^2-1\right)\left(N_J^g\right)^{-2}+\frac{5}{3}\left(N_J^\beta\right)^2\right] - 2d^2C_{202}^{J'2J}\sum_{J_1}\frac{1}{2J_1+1}C_{000}^{J2J_1}C_{2-20}^{J2J_1}\left(N_{J_1}^g\right)^2\right\}, \tag{C.5}$$

$$\langle\phi_J^\gamma||Q_2^h||\phi_{J'}^\gamma\rangle = q_h\left[1+\frac{\hat{J}'}{\hat{J}}(-)^{J'-J}(J'\leftrightarrow J)\right]\langle\phi_J^\gamma||b||\phi_{J'}^\gamma\rangle, \tag{C.6}$$

$$\langle\phi_J^\gamma||b||\phi_{J'}^\gamma\rangle = d(2J'+1)N_J^\gamma N_{J'}^\gamma\left\{\frac{1}{2J+1}C_{202}^{J'2J}\left(N_J^\gamma\right)^{-2} + \sum_{J_1}C_{2-20}^{J'2J_1}W(J'2J_12;J2)\left[2\sqrt{\frac{2}{7}}\frac{\hat{2}}{\hat{J}_1}C_{0-2-2}^{J_12J}\left(N_{J_1}^\gamma\right)^{-2} + 20\sum_{J_2}\frac{\hat{J}_1}{\hat{J}_2}C_{000}^{J_12J_2}C_{0-2-2}^{J_22J}W(J2J_22;J_12)\left(N_{J_2}^\gamma\right)^{-2}\right]\right\}. \tag{C.7}$$

The exact expressions for the m.e. of the anharmonic quadrupole transition operator are the following [5]:

$$\langle\phi_J^g||Q_2^{anh}||\phi_{J'}^g\rangle = -q_1d^2C_{000}^{J'2J}\left[\frac{2J'+1}{2J+1}\frac{N_{J'}^g}{N_J^g}+\frac{N_J^g}{N_{J'}^g}\right], \tag{C.8}$$

$$\langle\phi_J^\beta||Q_2^{anh}||\phi_{J'}^\beta\rangle = -q_1d^2C_{000}^{J'2J}\left[\frac{N_J^\beta}{N_{J'}^\beta}+\frac{2J'+1}{2J+1}\frac{N_{J'}^\beta}{N_J^\beta}\right], \tag{C.9}$$

$$\langle\phi_J^g||Q_2^{anh}||\phi_{J'}^\beta\rangle = -6\sqrt{\frac{1}{5}}q_1dC_{000}^{J'2J}\frac{N_J^gN_{J'}^\beta}{N_{J'}^g}, \tag{C.10}$$

$$\langle\phi_J^\gamma||Q_2^{anh}||\phi_{J'}^g\rangle = q_1N_J^\gamma N_{J'}^g\left[2\left(N_{J'}^g\right)^{-2}C_{022}^{J'2J}\left(1+\frac{2}{7}d^2\right) + 20d^2\hat{J}'\sum_{J_1J_2}\hat{J}_2C_{0-2-2}^{J_1J_2J}C_{000}^{J_12J'}C_{022}^{22J_2}T_{J_1J_2}^{JJ'}\right], \tag{C.11}$$

$$\langle\phi_J^\beta||Q_2^{anh}||\phi_{J'}^\gamma\rangle = \frac{q_{anh}}{q_h}\left[\frac{6}{\sqrt{5}}\langle\phi_J^g||Q_h||\phi_{J'}^\gamma\rangle\frac{N_J^\beta}{N_J^g} + 2d\hat{2}\sum_{J_1}\hat{J}_1C_{000}^{J_10J}W(22JJ';2J_1)\langle\phi_{J_1}^\beta||Q_h||\phi_{J'}^\gamma\rangle\frac{N_J^\beta}{N_{J_1}^\beta}\right]. \tag{C.12}$$

Author's personal copy

$$\langle\phi_J^\gamma||Q_2^{anh}||\phi_{J'}^\gamma\rangle = q_{anh}\left[1+\frac{\hat{J'}}{\hat{J}}(-)^{J'-J}(J'\leftrightarrow J)\right]\langle\phi_J^\gamma\|(bb)_2\|\phi_{J'}^\gamma\rangle, \tag{C.13}$$

$$\begin{aligned}\langle\phi_J^\gamma||(bb)_2||\phi_{J'}^\gamma\rangle \;=\; & N_J^\gamma N_{J'}^\gamma\left\{-\sqrt{\frac{2}{7}}C_{2\,0\,2}^{J'\,2\,J}d^2(N_{J'}^\gamma)^{-2}\right.\\ & +20d^2\sqrt{\frac{2}{7}}\hat{J'}\sum_{J_1J_2}\hat{J}_2C_{0-2-2}^{J_1\,2\,J'}C_{0-2-2}^{J_1J_2J}C_{0\,2\,2}^{2\,2J_2}T_{J_1J_2}^{JJ'}\\ & \left.+\;40d^2\hat{2}\hat{J'}\hat{J}\sum_{J_1J_2J_3}\hat{J}_2C_{2\,0\,2}^{2\,2J_3}C_{2\,0\,2}^{J\,J_2\,J_3}C_{0\,0\,0}^{J_1\,2\,J_2}C_{0-2-2}^{J_1\,2\,J'}S_{J_1J_2J_3}^{JJ'}\right\}.\end{aligned} \tag{C.14}$$

In the above equations, the following notations were used:

$$T_{J_1J_2}^{JJ'} = W(2222;2J_2)W(J'2J_1J_2;J2)\left(N_{J_1}^g\right)^{-2}, \tag{C.15}$$

$$S_{J_1J_2J_3}^{JJ'} = W(2222;2J_3)W(J_32JJ';2J_2)W(22J'J_2;2J_1)\left(N_{J_1}^g\right)^{-2}. \tag{C.16}$$

References

[1] A. Bohr, Mat. Fys. Medd. Dan. Vid. Selsk. 26 (1952) 14;
A. Bohr, B. Mottelson, Mat. Fys. Medd. Dan. Vid. Selsk. 27 (1953) 16.
[2] A. Faessler, W. Greiner, Z. Phys. 168 (1962) 425; 170 (1962) 105 ; 177 (1964) 190;
A. Faessler, W. Greiner, R. Sheline, Nucl. Phys. 70 (1965) 33.
[3] G. Gneus, U. Mosel, W. Greiner, Phys. Lett. 30B (1969) 397.
[4] P. Hess, J. Maruhn, W. Greiner, Phys. Rev. C23 (1981) 2335; J. Phys. G 7 (1981) 737.
[5] A.A. Raduta, V. Ceausescu, A. Gheorghe, R.M. Dreizler, Phys. Lett. 99B (1981) 444; Nucl. Phys. A381 (1982) 253.
[6] A.A. Raduta, V. Ceausescu, A. Faessler, Phys. Rev. C36 (1987) 2111.
[7] A.A. Raduta, C. Lima, A. Faessler, Z. Phys. A 313 (1983) 69.
[8] A.A. Raduta, Al.H. Raduta, A. Faessler, Phys. Rev. C55 (1997) 1747;
A.A. Raduta, D. Ionescu, A. Faessler, Phys. Rev. C65 (2002) 064322.
[9] A.A. Raduta, Recent Res. Devel. Nucl. Phys. 1 (2004) 1–70.
[10] L. Wilets, M. Jean, Phys. Rev. 102 (1956) 788.
[11] A.S. Davydov, G.F. Filippov, Nucl. Phys. 8 (1958) 788.
[12] A. Arima, F. Iachello, Ann. Phys. NY 99 (1976) 253; 123 (1979) 468.
[13] F. Iachello, A. Arima, The Interacting Boson Model, Cambridge University Press, Cambridge, England, 1987.
[14] F. Iachello, Phys. Rev. Lett. 85 (2000) 3580.
[15] F. Iachello, Phys. Rev. Lett. 87 (2001) 052502.
[16] A.A. Raduta, R. Budaca, A. Faessler, J. Phys. G: Nucl. Part. Phys. 37 (2010) 085108.
[17] R.K. Sheline, Rev. Mod. Phys. 32 (1960) 1.
[18] M. Sakai, Nucl. Phys. A104 (1967) 301; Nucl. Data Tables A 8 (1970) 323; A10 (1972) 511.
[19] A.A. Raduta, A. Gheorghe, M. Badea, Z. Physik A 283 (1977) 79.
[20] A.A. Raduta, Rev. Roum. Phys. 28 (3) (1983) 195.
[21] A.A. Raduta, S. Stoica, N. Sandulescu, Rev. Roum. Phys. 29 (1) (1984) 55.
[22] A. Gheorghe, A.A. Raduta, V. Ceausescu, Nucl. Phys. A296 (1978) 228.
[23] A.A. Raduta, A. Gheorghe, V. Ceausescu, Nucl. Phys. A311 (1978) 118.
[24] A.A. Raduta, S. Stoica, N. Sandulescu, Rev. Roum. Phys. Tome 29 (1) (1984) 55.
[25] G. Alaga, Nucl. Phys. 4 (1957) 625.
[26] M.E. Rose, Elementary Theory of Angular Momentum, Wiley, New York, 1957.
[27] A.A. Raduta, C. Sabac, Ann. Phys. 148 (1983) 1.
[28] A.A. Raduta, A. Faessler, J. Phys. G (2005); Nucl. Part. Phys. 31 (2005) 873.
[29] A.A. Raduta, P. Buganu, Phys. Rev. C83 (2011) 034313.
[30] Lo Iudice, A.A. Raduta, D.S. Delion, Phys. Rev. C 50 (1994) 127.
[31] F. Iachello, Phys. Rev. Lett. 91 (2003) 132–502.
[32] D. De Frenne, E. Jacobs, NDS 83 (1998) 535.
[33] J. Katakura, K. Kitao, NDS 97 (2002) 765.
[34] A. Artna-Cohen, NDS 79 (1996) 1.
[35] C.W. Reich, R.G. Helmer, NDS 85 (1998) 171.
[36] B. Singh, NDS 95 (2002) 387.
[37] B. Singh, NDS 99 (2003) 275.
[38] C.M. Baglin, NDS 84 (1998) 717.
[39] B. Singh, R.B. Firestone, NDS 74 (1995) 383.

Author's personal copy

[40] C.M. Baglin, NDS 99 (2003) 1.
[41] E. Browne, B. Singh, NDS 79 (1996) 277.
[42] Z. Chunmei, W. Gongqing, T. Zhenlan, NDS 83 (1988) 145.
[43] G.A. Lalazissis, S. Raman, P. Ring, At. Data Nucl. Data Tables 71 (1999) 140.
[44] C.W. Reich, NDS 91 (2003) 753.
[45] R.G. Helmer, NDS 101 (2004) 325.
[46] C.W. Reich, NDS 78 (1996) 547.
[47] R.G. Helmer, NDS 87 (1999) 317.
[48] A. Artna-Cohen, NDS 80 (1997) 723.
[49] J. Gröger, T. Weber, J. de Boer, H. Baltzer, K. Freitag, A. Gollwitzer, G. Graw, C. Günter, Acta Phys. Pol. 29 (1998) 365.
[50] Y, A. Akovali, NDS 69 (1993) 155.
[51] M.R. Schmorak, NDS 63 (1991) 139.
[52] Y, A. Akovali, NDS 71 (1994) 181.
[53] M.R. Schmorak, NDS 63 (1991) 183.
[54] F.E. Chukreev, V.E. Makarenko, M.J. Martin, NDS 97 (2002) 129.
[55] F.E. Chukreev, Balraj Singh, NDS 103 (2004) 325.
[56] Y, A. Akovali, NDS 96 (2002) 177.
[57] Y, A. Akovali, NDS 87 (1999) 249.
[58] E. der Mateosian, J.K. Tuli, NDS 75 (1995) 827.
[59] R.G. Helmer, C.W. Reich, NDS 87 (1999) 317.
[60] B. Singh, NDS 93 (2001) 243.
[61] E.N. Shurshikov, N.V. Timofeeva, NDS 67 (1992) 45.
[62] B. Singh, NDS 75 (1995) 199.
[63] E. Browne, Hou Junde, NDS 87 (1999) 15.
[64] E. Browne, Hou Junde, NDS 84 (1998) 337.
[65] E. Browne, NDS 72 (1994) 221.
[66] M. Finger, et al., Nucl. Phys. A188 (1972) 369.
[67] U. Meyer, A.A. Raduta, A. Faessler, Nucl. Phys. A 637 (1998) 321.
[68] A.A. Raduta, P. Buganu, Phys. Rev. C83 (2011) 034313.